RADIOMETRIC CORRECTIONS THROUGH WHITE REGION NORMALIZATION

by

John Patric MacDonald

B.A. Simon Fraser University 1987

THESIS SUBMITTED IN PARTIAL FULFILLMENT OF THE REQUIREMENTS FOR THE DEGREE OF MASTER OF SCIENCE (GEOGRAPHY)

in the Faculty

of

Arts

SIMON FRASER UNIVERSITY

NOVEMBER 1989

APPROVAL

Name: John Patric MacDonald

Degree: Master of Science

Title of Thesis: Radiometric Corrections Through White Region Normalization

Examining Committee:

Chairman: I. Hutchinson, Associate Professor

A.C.B. Roberts
Associate Professor
Senior Supervisor

R.B. Horsfall
Assistant Professor

S. Kloster
Computing Services
Simon Fraser University

B. Beyerstein
Associate Professor
External Examiner
Department of Psychology
Simon Fraser University

Date Approved: November 29, 1989

PARTIAL COPYRIGHT LICENSE

I hereby grant to Simon Fraser University the right to lend my thesis, project or extended essay (the title of which is shown below) to users of the Simon Fraser University Library, and to make partial or single copies only for such users or in response to a request from the library of any other university, or other educational institution, on its own behalf or for one of its users. I further agree that permission for multiple copying of this work for scholarly purposes may be granted by me or the Dean of Graduate Studies. It is understood that copying or publication of this work for financial gain shall not be allowed without my written permission.

Title of Thesis/Project/Extended Essay

Radiometric Corrections Through White Region Normalization

Author: _____
(signature)

John Patric MacDonald
(name)

feb. 5 / 90
(date)

Abstract

Recent developments in color vision theory have produced models of how humans extract lightness and color information under conditions of graded illumination. Certain aspects of these models can be useful in correcting radiometric distortions inherent in remotely sensed digital images.

A white region normalization algorithm designed to approximate a condition of even illumination in accordance with human color vision theory, was tested for its utility in remote sensing applications. The algorithm design evolved from the principles outlined by Land's (1977) publication of retinex theory. Color target conditions included: graded illumination, specular reflectance, and mixtures of dominant wavelengths in illuminants. The algorithm was separately applied to each of the (red, green, and blue) spectral wavebands.

A series of thresholds associated with between point ratios, accompanied by iterative procedures, were tested for their performance. Results indicated that the algorithm performed well where illumination gradients were uniform and/or varied gradually. When compared with standard image enhancement techniques, applied in the processing of digital remote sensing images, white region normalization provided a promising alternative.

ACKNOWLEDGEMENTS

The author wishes to express sincere appreciation to professors A.C.B. Roberts and R.B. Horsfall for their assistance in preparing this manuscript. Special thanks are due to Dr. S. Kloster for his help in developing the program and professor B. Beyerstein, external examiner.

TABLE OF CONTENTS

List of Tables

List of Figures

I

INTRODUCTION

Human beings evolved in a world filled with colors. The progress of human evolution has resulted in the average observer being able to discriminate some 5,000,000 colors and 200 shades of gray. The entire content of our visual world is a creation of complex mechanisms and robust processes between the inner eye and cerebral cortex of our brain.

Color is without exception an extremely important indicator in the day-to-day activities of life. Throughout each day, our world is illuminated by varying intensities of direct sunlight, diffuse skylight, flame and a variety of artificial light sources. In spite of the changes and varying gradients of illumination in our world, object colors remain largely unchanged for us. One can easily understand the importance of such a feature whether in the natural environment of early hunter gatherers or in a busy urban setting filled with the hazards of automobile traffic.

For hundreds of years artists, philosophers and scientists have endeavoured to solve the mysteries behind human color vision processes and in recent years there has been a revived interest in the subject. Developments

in artificial intelligence and robotics have rekindled investigations into how humans extract lightness and color information under conditions of graded and changing illumination. Investigators in these fields are more interested in the visual processes involved than in the end results. The remote sensing community, specifically the image analyst is, however, more interested in the end product of color information extraction from graded illumination than in the process.

Remote sensing is the science, art and technology of extracting earth's resources information remote from the subject of investigation. In doing so a variety of imaging techniques is employed. From multiband photography, which was first used during the 1950's and later taken into space by the NASA space program, to the newer multispectral scanners and array scanners, none have the dynamic capabilities of human vision. The similarity between multispectral sensors used in remote sensing and the photosensitive cells of the human eye is that both have imaging capabilities tuned to discrete spectral wavelength regions (band widths). The sensors within the human eye differ mainly in the width and overlap of their spectral sensitivity (Fig. 1-1). However, the most important difference is the dynamic ability of the human eye to image scenes without the perceived colors being affected by shifts in wavelength

Fig. 1-1.

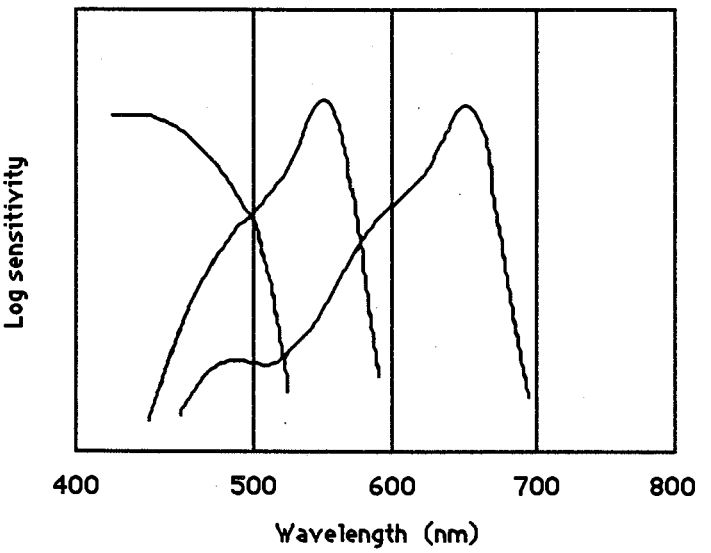

Spectral sensitivity curves of color film.
[As taken from Lillesand and Kiefer, (1979)]

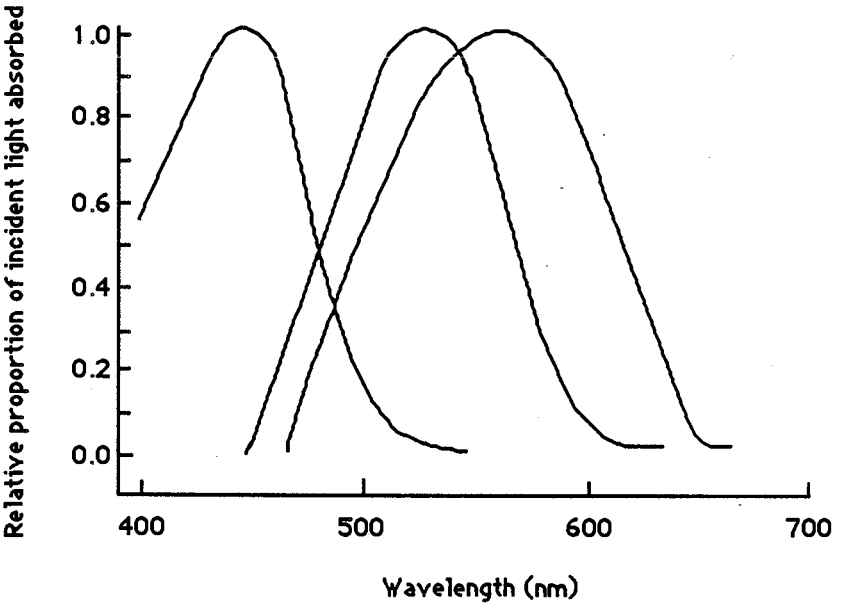

Absorption spectra for the three classes of cones found in the human retina. Heights have been adjusted to have maxima at 1.0 [As taken from Cornsweet, (1970)]

and light flux. It is this difference in dynamic abilities that represents an important problem to be overcome by the remote sensing community.

The problem is to extract the true reflective and absorptive characteristics of the target being imaged. This process can be termed "radiometric filtration". It is accomplished by applying mathematical equations in a computerized format. Digital values can be generated for multiband photographic images as well as electronically generated scanner images. Once recorded in their digital formats, the basic units of an image are displayed as gray tone values which are similar to the single photoreceptor images produced by the human eye. Discrete gray tones represent both spatial and spectral information recorded for an imaged scene.

The purpose of this study was to determine the utility of using a mathematical model, developed from theories of how humans extract lightness and color information from unevenly illuminated scenes, in correcting radiometric distortions inherent in remotely sensed scenes recorded under conditions of uneven illumination. The study included the use of photographic film for recording target conditions and a computer analysis of the gray tone information from color separations which were video digitized.

A color target which has been subjected to graded illumination at two angles (from beneath and overhead) was employed. Tungsten and mercury vapor lamps provided the light sources which generated color shifts in the resulting photographic image.

The photographic image was then digitized as color separations wherein the red, green and blue emulsions are represented as an array of gray tones with integer values. The digital arrays for each wave band were processed separately on a large mini computer using software developed for testing the algorithm selected. The algorithm used in the test was based upon the work of the human color vision theorist, Edwin Land. Once corrected, the separate spectral bands were displayed in an additive manner as a reconstructed color image and displayed on a video monitor. The corrected images were analyzed to assess the utility of the correction using standard image analysis techniques.

The general assumptions accepted from the outset are included within the body of knowledge embraced by human color vision theory. These include: 1. brightness constancy, wherein the apparent brightness of an object tends to remain constant despite changes in illumination; 2. edge detection, and the importance of edges in initiating contour perception over visual fields; 3. lightness ratios, object color depending on the ratios of

light reflected from the visual field rather than the absolute amount of light; 4. relative excitation, the basic information about color as we perceive it being derived from the relative degree of excitation between the individual wave bands of the long, medium and short band (red, green and blue) photo receptors, and; 5. color constancy, wherein perceived color appears constant despite changes in wavelength of the source of illumination. Land's theory from which the basic algorithm for testing was developed, embraces all of these well-accepted notions.

The general approach was to apply a version of the basic algorithm as described by Land in his 1977 publication on Retinex Theory. Tests included applying the algorithm to the three separated digital images representing the red, green and blue filtration bands of the color target. A series of threshold values, as well as iterative procedures, were tested for comparison and analysis. Image profiles and photographic color plates were produced upon processing the images and used in assessing the different results achieved by varying the threshold and iterative parameters. Should the correction procedure result in the removal or reduction of the illumination gradient and improved color definition, leading to more reliable classification of target regions, it can be concluded that the Retinex

"radiometric filtration" corrects for variations in object brightness, permitting identification of object color with some independance from electromagnetic energy flux. This type of correction, if reliable, would substantially improve target identification when processing digital images.

II

THEORY

The theoretical basis underlying this project will be addressed by component. Land's retinex theory of light perception is the departure point for the experimental approach taken and will be discussed first. The theoretical background of the underlying assumptions of brightness constancy; edge detection; lightness ratios; relative excitation, and; color constancy will be examined for their relevance, in relation to retinex theory and the experimental methods applied.

Retinex Theory (Land 1964;74;77;86, Land and McCann 1971) describes an analytical course through which the human visual system could process images for color vision. The process provides a method of radiometric filtration which corrects for variations in true object brightness and perceived lightness, permitting the identification of object reflectivity and absorption characteristics with some independence from electromagnetic energy flux.

Land's 1977 theory assumed three sets of photoreceptor cells called cones for their shape. Of the one hundred million photosensitive cells in the human eye some six to seven million are cones (Brown and Wald ,

1963:64). Their broadly overlapping bands have absorption peaks near 440, 535 and 565 nm (Land, 1977). The nanometer (nm) is the unit commonly used in specifying the wavelength of visible radiation (MacAdam, 1985). Wavelength as measured by a spectrophotometer is an unambiguous and accurate measure of hue (and can also be of "color"). Color specification can also be made in terms of tri-stimulus values. The tri-stimulus values of the three color primaries red, green, and blue (X Y Z) can be combined to match the color at each wavelength of an equal energy spectrum (Manual of Remote Sensing, 1975).

The first stage of the visual process begins when light reflected from an object or objects enters the eye. Upon absorbing quanta, the cone cells respond to the bleaching of their photo-sensitive pigment with neural signals (Cornsweet, 1970).

Land (1964;74;77;86) asserted that color sensation results from a comparison of excitations between cone sets affected by each point in a scene, starting with a reference point. In fact, as long as the comparison includes the reference point, it need not be the starting point. The reference point is the point in the scene with the highest "integrated reflectance" in all three receptor sets and may be considered analogous to a bench mark to which the lightness of all other perceived

objects is calibrated. In most if not all images, objects having the highest integrated reflectance in all three receptor sets will result in the perception of white. Land's theory asserts that the final perceptual response of the visual system is lightness * (Note: " The attribute of object colors by which the object appears to reflect or transmit more or less of the incident light. " Webster's Seventh New Collegiate Dictionary.)

Herein, lightness and apparent brightness * are considered to be synonyms. (Note: " Radiating or reflecting light. " Webster's Seventh New Collegiate Dictionary.) Of the three broad spectral bands suggested by Land each has its own characteristic response to the light stimulus of a scene. For instance objects reflecting blue light have their highest reflectance or appear brightest in the blue band, their mid-range reflectance in the green band, and their lowest reflectance in the red band. Similarly objects reflecting red light have their highest reflectance in the red band, their mid-range and lowest reflectance in the green and blue bands respectively.

This phenomenon can be readily observed by viewing colored objects in a scene through red, green, and blue photographic filters. Retinex theory proposes that while the signal produced in the outer segment of the photoreceptor cell seems to be proportional to the light

flux absorbed by the visual pigment, the end response of the visual system is lightness (Land, 1959;1977). Land arrived at this conclusion by testing the perceptual sensations of dark adapted subjects. After complete dark adaption, a natural scene was illuminated to a level sufficient to stimulate only the hypersensitive photoreceptor system known by their shape as rods. Subjects reported a colorless world where objects were characterized by various tones of lightness from white to black. The lightness of each object of the colorless image was not directly determined by the flux of radiant energy reaching the eye when one varied the illumination throughout the scene. Reports from subjects indicated that objects and background retained their characteristic lightness regardless of changes in illumination. For example a dark grey or black object reflecting more light than a white object would still be seen as dark while the white object would be correctly perceived as being white.

Results of experiments conducted by Land and McCann (1971) indicated that color perception is partially independent from electromagnetic energy flux (changes in the rate of energy flow across an object or scene) and wavelength. This observation is confirmed by everyday life experiences. Daylight is traditionally the source by which objects are examined for their color because it contains a mixture of nearly all components of the

visible spectrum in near equal proportions (MacAdam, 1985). Throughout our day observable scenes in our world are subjected to changes of light flux and wavelength. Frequent changes in atmospheric conditions result in different types of light scatter. These changes are manifest in the form of clouds, fog and haze which are continually changing light flux and causing shifts in dominant wavelength.

Light sources such as daylight fluorescent lamps may have the same correlated color temperature as some phase of natural daylight but the spectral distribution of power (dominant wavelength) of the artificial source will differ greatly (MacAdam, 1985). As we pass through a variety of lighting conditions from skylight, which changes in flux and wavelength with each passing cloud, into artificial lighting, which varies considerably in dominant wavelength, our perception of color remains largely unchanged. Unlike other imaging sensors only the living eye is presently capable of seeing the world in this way. Photographic film, for instance, is not so versatile. Although constructed in such a way as to replicate scene colors, film is highly affected by shifts in wavelength. This is readily demonstrated when using daylight color film indoors without the proper flash attachment. Where the scene or object photographed is illuminated by incandescent tungsten light, the resulting

photograph will appear yellow as a result of the dominant wavelength of the lighting. Similarly if the photograph were taken under fluorescent lighting the resulting photograph would be greenish in appearance as a result of the dominant wavelength emitted by the excited fluorescent tube.

What makes the human visual system capable of recording true object lightness? According to Land (1977) each cone system (ie: red, green and blue) integrates for each point in a given scene the influence of the light of all wavelengths to which the (R G B) cone is sensitive, then compares the degree of excitation of the cones that encode the same color at the reference point. He speculated that the human visual system arrives at a given color sensation through the comparison of the three (R G B) lightness sensations on a point by point basis and this information is processed somewhere between the retina and the cerebral cortex of the brain. He termed the three comparator systems retinexes.

Land has provided several arithmetic models, illustrating how such a comparison can be made, in his 1977 model. The point by point comparison is made by ratioing the reflected brightness between two neighbouring points and scaling the resulting quotient to a reference point. Once all points within a scene have been scaled to some corresponding reference point, the

integrated reflectance for all points in the object scene has been established. This process is repeated for each waveband corresponding to the red, green and blue cones.

Threshold Test

Each ratioed neighbouring point pair is further subjected to a threshold test to establish whether an object edge or actual change in reflectance exists as opposed to gradual changes in illumination caused by light gradients. Thresholding techniques have been applied in various forms in image analysis and processing (Perkins, 1980; Canny, 1986; Pitas and Venetsanopoulos, 1986). The technique normally applied compares the brightness value of each pixel to a predefined threshold value then assigns the pixel to one or more categories depending upon whether the threshold value is or is not exceeded. Threshold values are often chosen on the basis of image histograms. An image consisting predominantly of two regions (light and dark) will exhibit two distinct peaks in its histogram. Such an image is considered bimodal. In such a case threshold values are selected from within the region between the two peaks (Pavlidis, 1982). Images histograms are rarely as distinctive as this, hence threshold selection is often somewhat more complicated and can be very sensitive.

Land (1977) asserted that the procedure of taking the ratios between two adjacent points can detect an object edge and thresholding can eliminate the effect of non-uniform illumination (Fig. 2-1). The threshold operator will determine whether the relationship between two points constitutes the existence of an edge or graded light. The ratios represent the reflectance at the edge between two adjacent areas while the integrated reflectance represents the relation of all ratios of reflectances in the field of view (eg; every point ratioed with every other point). The values obtained after multiple iterations of the procedure are the integrated reflectance expressed as a percentage of the brightest value which, is white.

This procedure may be seen as analogous to radiometric filtration which corrects for variations in object lightness to approximate a condition of even illumination. This permits the identification of original object color (reflectivity-absorption characteristics) independently from electromagnetic energy flux variations. The results of Land's experiments suggested that it is possible to use a version of this model in software format as a pre-processing filter to correct for changes in ambient flux in remotely sensed images.

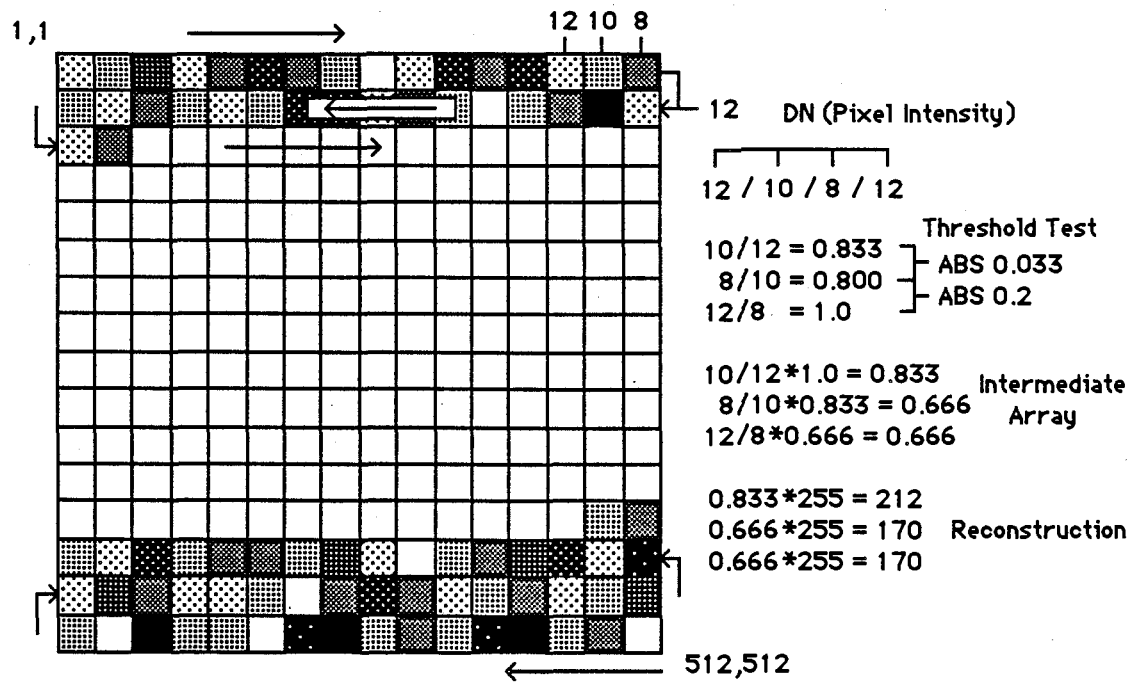

Fig. 2-1. Diagram illustrating ratioing method used upon original pixel intensities (DN), threshold test, intermediate array, and reconstruction ready for display or reiteration.

Image Filtering

Filtering, in the domain of image spatial and spectral frequency transform, is highly analogous to some models of human perception. It involves a compromise between image sharpness and noise in its operations (Manual of Remote Sensing, 1983). Spatial filters for remotely sensed digital images are defined by their shape, size, and implementation procedure. These two parameters are related to the number and configuration of lines and samples (pixel coordinates) that overlay a progressively indexed portion of an image (Manual of Remote Sensing, 1983). Different shapes, sizes, and procedures obtain different results. Larger rectangular or square filters tend to enhance low spatial frequency features while attenuating the noise associated with higher spatial frequencies. Conversely, smaller filters of this type have the opposite effect and emphasize edges. An increase in image contrast results with the increase in intensity of high spatial frequencies associated with edge enhancement. The retinex type filter employed for this project belongs to the edge enhancement category and is intended to emphasize high spatial frequencies.

Atmospheric Effects

Atmosphere is a very important factor affecting color constancy and the interpretation of remote sensing imagery. In recent years researchers have produced a number of valuable models outlining the atmospheric parameters affecting remotely sensed data (Niple, 1980; Gordon and Clark, 1981; Kopeika, 1982; Kaufman, 1981,82,84; Fraser and Kaufman, 1985; Chu, 1982; Horn, 1983; Dechamps, Herman, and Tanre, 1983; Diner and Martonchik, 1985; Pearce, 1985; Woodham and Gray, 1987). Atmospheric scattering of reflected light imaged by passive sensors, both airborne and orbital, reduces image contrast across edges. The effects are similar where human visual airborne observations are concerned. One may safely assume that under orbital conditions the same effects would also prevail for a human observer. The amount of contrast degradation depends on object shape and size as well as atmospheric characteristics (Kaufman, 1981,82,84; Kopeika, 1982; Diner and Martonchik, 1985). Kaufman (1981) modelled the effects of earth's atmosphere on visibility in the nadir direction as determined by the human eye. He noted that, within limits, the intensities are nearly linear and decrease with distance from the border between two areas of high contrast in a gray tone image.

The United States Geological Survey, (1979) developed a model for correcting the first order effects

for atmospheric scattering (haze) establishing an offset ("dark object subtraction") corresponding to the amount of increase to be subtracted per gray level for each spectral band (Manual of Remote Sensing, 1983). Although successful results for atmospheric modelling have appeared in the literature, the most promising of these are based upon simulations restricted to aerosol distributions of finite scales (one and ten kilometers) and do not adequately account for angle of illumination and variations in electromagnetic energy flux when combined with the non-uniform reflectance of the earth's surface (Kaufman, 1981,84; Gordon and Clark, 1981).

Okayama and Ogura, (1983) have developed a promising method of obtaining an indicatrix (scattering diagram) of the earth's surface over beach sands and urban areas through remote sensing simulations, yet a myriad of other landscapes remain unmodelled. The authors chose these two surface types because they show only small variations in spectral reflectance over finite time periods (one year). Sjoberg and Horn (1983) modelled the atmospheric effects in satellite imaging of mountainous terrain with interesting conclusions. Lacking ground truth for comparison, they generated albedo maps of surface reflectances under very generalized terms. The authors point out that more exact models of the radiative transfer process require exact description of surface

reflectance in order to extract surface reflectance information. The human image interpreter, however, does not dynamically solve the radiative transfer equation when interpreting images but applies a more intelligent technique (Sjoberg and Horn, 1983). Still yet to be accomplished is a successful marriage of atmospheric and surface modelling techniques, which parallel the performance of the human interpreter. For the time being radiometric distortion due to atmospheric effects remains as a critical and largely unsolved image correction problem.

Dark Object Subtraction

The correction of remotely sensed digital data without outside information (eg; atmospheric parameters collected at the time of imaging or modelled on assumptions) can be accomplished by dark object subtraction. The idea involves subtracting the gray tone difference between the lowest reflective body in a scene and zero from all gray tones in the scene. The assumption here is that the body with the lowest reflectivity in a scene in a single band of the visible spectrum would approximate the radiative characteristics of a blackbody if not for the additive effect of atmosphere. This technique is widely used and has been combined with more sophisticated methods using

atmospheric transmission models requiring detailed field data which generally are not available.

Chavez, (1988) has provided a recent improvement on the traditional method of dark object subtraction. Using information supplied by Curcio (1961) and Slater et al. (1983), Chavez (1988) developed relative scattering models based upon power functions associated with generalized atmospheric conditions. This model requires correction for "gain" and "offset" of the type of imaging system used plus correction for the multiplicative and additive terms of a computed radiance value for each pixel coordinate. Computation for radiance values requires generalized surface slope information for each coordinate pair as well. This factor restricts the use of this model where, for example, airborne video systems are concerned and second generation images such as video digitized aerial photographs as the parameters (gain and offset) are not readily obtainable for these data.

Although some aspects of this model provide insight towards improving traditional dark object subtraction methods, other aspects are computationally burdensome for a model based upon many generalizations. As a generalized model a retinex type correction should perform as well as dark object subtraction in eliminating the effect of atmospheric scatter by correcting for

changes in ambient flux in remotely sensed digital images.

Assumptions of Retinex Theory

Although not explicitly stated by Land (1959;1977) retinex theory embraces five of the well-accepted attributes of human color vision performance. These are: [1] brightness constancy; [2] edge detection; [3] lightness ratios (in hue perception); [4] relative excitation, (between wavebands or cone sets), and; [5] color constancy.

Brightness Constancy

Brightness constancy simply means that the apparent brightness (lightness sensation) of an object tends to remain constant despite changes in illumination falling on it (Cornsweet, 1970). Various researchers (Land, 1959;1977; Graham, 1965; Cornsweet, 1970; Boynton, 1979; Brou, Sciascia, Linden and Lettvin, 1986), have observed and noted this phenomenon. For example, an ordinary piece of white paper reflects about 90% of the incident light while black paper reflects about 10% when viewed in ordinary room light. When viewed in direct sun light the increase in intensity may be 1000-fold yet the papers retain their apparent relative brightness compared to when they were viewed indoors (Cornsweet, 1970).

A procedure often used to measure brightness constancy involves a subject viewing an array of gray papers ranging from black to white with the illumination held constant. Subjects are required to match from the series of gray papers a test patch which is simply another piece of gray paper. The shade and intensity of illumination of the test patch and its surroundings are varied yet the subjects almost always choose a matching gray that is physically the same as the test patch (Cornsweet, 1970).

It is interesting to note that most subjects show only minor departures from perfect brightness constancy. Exceptions do arise if the illumination is confined to the illuminated patch alone, excluding the background and surrounding area. Under these circumstances no constancy is shown (Cornsweet, 1970). Upon examining data collected by Heinemann (1955), Cornsweet (1970) concluded that an object's lightness or apparent brightness depends not only on the intensity of light falling on the retinal image of a point, but more importantly upon the relations between the intensities within the overall field of view. He further concluded that lightness or apparent brightness at each point is determined by the intensity distribution in a region that includes both the point and its surrounding area.

Stiehl, McCann and Savoy (1983), in examining the influence of intraocular scatter on lightness scales, also found that lightness is a function of both luminance at a point and spatial interactions with other points in the field of view. In terms of physical contrasts of retinal images, intraocular media scatter light from high luminance areas into low luminance areas, while in terms of apparent contrasts (sensation) white (high luminance) surrounds make gray patch (low luminance) areas darker rather than lighter. The first phenomenon is one of physical light scattering while the second is performed by a neural contrast mechanism. The lack of perfect cancellation of the two opposing phenomena results in the phenomenon known as simultaneous contrast. This phenomenon is integral to hue (color) constancy as well as brightness constancy and will be discussed further with respect to color constancy.

It becomes apparent when examining the phenomenon of brightness constancy in the context of retinex theory that Land (1964;74;77;86) embraced this notion in his conclusion that the "white" reference point is the point in the scene with the highest integrated reflectance in all three receptor sets and may be considered analogous to a bench mark to which the lightness of all other objects in the field of view are compared or calibrated. The key notion is that of integrated (to make whole by

bringing together all necessary parts) reflectance. The apparent brightness of any point in an object scene is relative to the lightest point (white reference point) in the field.

Horn (1974) concurs with the assumption that the highest lightness value corresponds to white is the best one can do. Other normalization techniques (adjusting weighted local averages) would not amount to a reconstruction of reflectance, particularly where the light source in the field of view contains fluorescent colors or specular reflections.

Land's (1977) model for integrated reflectance accounts for the intensity distribution between points by representing the relation of all ratios of reflectances in the field of view. In doing so his procedure provides an analytical tool that simulates brightness constancy.

Edge Detection

The significance of edge detection in human vision was noted by Da Vinci and demonstrated by Ernst Mach in 1865 (Graham, 1965). Mach noted that if two juxtaposed uniform surfaces are seen as reflecting different amounts of light the border between them appears to be lighter than the area on the side of the lighter of the two. More recent works (Boynton, 1979; Marr, 1982) in the field of human color vision have noted as well the

importance of edges in initiating contour perception over visual fields.

Kaufman (1981) in his description of Overington's (1971) model of vision points out that the visual detection of a change in illuminance across a field is determined by the neural response to the "maximal illuminance gradients" of the image on the retina. He notes that detection is performed in the brain "through a comparison of the responses of adjacent pairs of reportors (retinal cells that detect edges) across the edge of the image". Overington and Levin (1971) developed a formula for calculating the contrast threshold of visibility upon which detection was dependent (Kaufman, 1981).

The visual world is comprised of contours, creases, breaks, marks, shadows and shading, all of which are spatially localized (Marr, 1982). Marr (1982) points out that these are the properties which give rise to intensity changes in an image. Marr (1982) avoids using the term edge as it implies a physical boundary and rather prefers the term intensity changes. Graham (1965), Land (1977) and Boynton (1979) suggested that the term "edge" implies changes in intensity that are not within the limits of illumination gradients and therefore represent changes in the physical properties of object reflectance. Illumination gradients are usually small

and linear (Marr, 1983). Land (1977) also provided a mechanism for edge detection through applying a pre-defined threshold test to between point ratios.

Segmenting images into abrupt intensity changes is often considered a necessary aid to interpretation. A great deal of interest in this task has arisen in the field of artificial intelligence as it relates to image analysis. A great deal of two and three dimensional information lies in the detection of image edge points. Various techniques have been developed involving different levels of complexity (Perkins, 1980; Pitas and Venetsanopoulo, 1986; Canny, 1986; and Bergholm, 1987).

Perkins (1980) points out that the seemingly simple goal of separating images into uniform intensity regions is difficult to implement because such regions are only approximately uniform and their boundaries are not always distinct and contain gaps. Perkins (1980) developed an improved edge point detection method which avoided the merging of dissimilar regions caused by edge boundary gaps by expanding edge regions; enlarging detail to close gaps then contracting boundaries by reversing the technique after separation. Employing a progressively indexed nine pixel kernel, edge pixels were separated into two classes, horizontal or vertical by comparing gradient (edge magnitude) and direction.

Small uniform intensity regions less than ten pixels in size were merged into the surrounding edge region resulting in a loss of fine detail. His method also failed where gaps between edge points were too large for his operator and intensities varied slowly with surface curvature providing too few edges.

Marr (1982) and Canny (1986) evaluated Gaussian type operators similar to the Perkins (1980) operator. Gaussian filters smooth edges in both the spatial and frequency domains and are often used as the first step in detecting intensity changes in images (Marr, 1982). Marr (1982) and Canny (1986) indicated that the more successful methods of edge detection involve using some derivative of a Gaussian filter by estimating the slope (first derivative) or rate of change of the slope (second derivative) of the illumination gradient.

Using this technique, numerical values in the resulting filtered image can be "binarized". White regions can be represented by positive values and black regions by negative values with average (intermediate gray) values being zero. Zero crossings mark intensity changes and when displayed alone clearly mark the edges dividing intensity regions. The slope of the zero crossings when measured perpendicular to their local orientation, which are roughly uniform, depends on the contrast of the intensity change. Resulting edges are

normally displayed as closed contours (Marr, 1982). Canny (1986) experimented further with Gaussian convolutions providing criteria for modifications for similar types of edge detectors.

Pitas and Venetysanopoulos (1986) compared various edge detectors based on nonlinear computational "filters" and found that they performed well where noise was uniformly distributed. They concluded that detectors based on median, order statistics, and nonlinear filtering were more promising providing speed and good noise removal characteristics. These measure the mean (arithmetic, geometric, harmonic, or contraharmonic) of the luminance. Their difference (choice of nonlinear mean) is based upon some measure of dispersion of illuminance within filter kernel extent. If greater than a certain threshold, then the center point is declared an edge point.

Bergholm (1987) added further refinement to edge detection with a method he termed edge focusing. As previously indicated, edge detection at a fine resolution yields noise and at a coarse resolution causes distortion and edge blurring. Bergholm (1987) suggests that these problems may be overcome through a coarse to fine tracking in a continuous manner. He also chose a Gaussian smoothing operator for his coarse operation and gradually refocussed image edges by continuously varying

toward a finer resolution. Using a subset of Canny's (1986) method, he combined good accuracy with good noise reduction results, improving overall the method. Bergholm's (1987) method was effective in removing to some extent diffuse edge contours caused by shadows and other illumination effects.

The above mentioned methods of edge detection are far more complex computationally than the modified between edge ratioing offered by Land's (1977) example employed herein. Land's (1977) method, however, used edge detection as a secondary or tertiary intermediate means to its overall end of approximating a condition of even illumination. It was determined for this reason, as well as for its merits of simplicity, that it should be further tested for remote sensing potential.

Lightness Ratios (Hue Perception)

Hue is the aspect of perception commonly called color (Cornsweet, 1970). Newton, in the latter part of the seventeenth century, found that sunlight could be analysed by refraction and thus could be displayed as a continuum of hues giving the impression of seven colors. These he named violet, indigo, blue, green, yellow, orange, and red (Paritsis and Stewart, 1983). Newton's findings were expanded upon by Young, Maxwell and

Grassman and later formed the foundation of Helmholtz's science of colorimetry (Evans, 1974).

Maxwell chose blue, green and red as his primary colors because within these spectral regions hue does not change dramatically. He also proved that white could be obtained by combining these primaries (Paritsis and Stewart, 1983). Helmholtz proposed that colors could be represented as a numerical function of three independent variables; luminosity (also referred to as brightness), hue, and saturation (Paritsis and Stewart, 1983).

The term luminosity or the quantity of white light reflected or projected was agreed upon by the International Commission on Illumination (1924) concerning relative luminances of equal amounts of energy at various wavelengths and it was adopted at the 1931 CIE meeting (MacAdam, 1985). The relative luminance of a sample is indicated by the ordinate (Y) value on a scale that is represented by absolute black as zero and a perfect white as one hundred (MacAdam, 1985). Put more generally, luminosity is the tristimulus value governing a color's brightness. Hue is the quantity of some color in the spectrum. The experiences, for example, of red, green, yellow, blue and blends of pairs of these are conventionally denoted as hue. Hue is generally considered to be a single dimension of one or more of these four color experiences (Boynton, 1979). Saturation

is the proportion of chromatic wavelength in the color. The "whiteishness" of a color is reduction of the dimension called saturation. For example a yellowish-white is termed a desaturated yellow; the more white a color appears to have in it the more it is said to be desaturated (Cornsweet, 1970).

Hue is the aspect that changes most strongly with changes in wavelength, brightness is the aspect that changes most strongly with changes in intensity and saturation is the aspect that changes chroma or purity of the hue (Cornsweet, 1970).

Thomas Young was the first to propose that the three primary colors corresponded to the sensitivity of our photo receptors (cones) and this was eventually demonstrated by Rushton (1961), Marks et al. (1964), Brown and Wald (1964), Paritsis and Stewart (1983). It is generally believed that, at some point early in the visual system, the ratios of the outputs of the three cone types are what is measured in maintaining hue constancy (Cornsweet, 1970). Cornsweet admitted that there is no convincing evidence that neural circuits exist which directly calculate ratios, although in principle, inhibitory functions performed between the retina and the neural pathways provide this capability.

This widely embraced view that object color depends upon the ratios of light reflected from various parts of

the visual field rather than the absolute amount of reflected light dates at least as far back as Ernst Mach (Marr, 1982). The phenomenon is known as simultaneous contrast. What this means is, simply, that changes in both lightness and hue are caused by the simultaneous presence of differing backgrounds (Boynton, 1979). Marr (1982) provides an elegant example of this phenomenon. Imagine a scene containing yellow and blue flowers growing amid a background of green grass and clover. The absolute amount of light coming from the flower cannot be relied upon as a clue to the surface reflectance characteristics of the flower, either in terms of lightness or its spectral properties. Its characteristics relative to other surrounding surfaces, however, are probably reliable.

Marr (1982) goes on to note that if relative measurements are to be relied upon, the distinction between changes in images due to changes in the reflectance function of an object and/or changes in illumination, must be made. For instance, a daisy in the shade looks darker than an unshadowed daisy but the shadowing does not affect the perceived color of the lawn or the daisy. Under both conditions the daisy still appears white (Marr, 1982).

Among modern color vision theorists (Helson, 1938; Judd, 1940; Cornsweet, 1970; Land and McCann, 1971;

Boynton, 1979; and Marr, 1982) the view that relative observations of lightness (apparent brightness) are what is relied upon in color perception, has stood the test of time. Retinex theory incorporates this notion in what Land (1977) termed integrated reflectance.

Shadows and the slope of the object surface provide the main sources of discontinuity in object brightness (Marr, 1982). The effect of the transformation when thresholding is applied to between edge ratios is to eliminate changes in illumination caused by light gradients (eg; shadows and slope of the object surface and/or the incident angle of the light source).

Relative Excitation

Having considered that the basic information about color perceived by the brain is derived initially from the relative degree of excitation of the three sets of photoreceptors (cones), some consideration must be given to the range of sensitivities of the cones. Boynton (1979), pointed out that the sensitivity range of the cones is under continuous adjustment over a range of luminance (intensity) of aproximately a million-to-one ($1x10^6$:1), with each eye doing so independently. He notes that some objects reflect more than 90% of their incident light no matter what the illumination. Those that reflect 70% or more appear white whether directly

viewed or seen in a photographic reproduction. At the other extreme, objects that reflect less than four or five percent of the incident light appear black. Under these circumstances the range of intensities that a photographic print must provide for adequate scene depiction need not be greater than twenty to one (20:1).

Photoreceptor (chromatic) adaptation is a complex process and a complete review is beyond the scope of this study. However, three of the mechanisms for adaptation are photopigment bleaching, pupilary constriction, and receptor response compression (Boynton, 1979). An accurate accounting of chromatic adaptation was outlined by von Kries's coefficient law of 1878. It stated that visual responses are proportional to the physical stimulation of each of the three receptor sets (cones) and that only the ratios of the coefficients of proportionality change from one chromatic adaptation to another (ie: the relative spectral sensitivities of any class of visual receptors do not change as a result of adaptation) (MacAdam, 1985). The consequence of the attribute of color vision called chromatic adaptation is color constancy (MacAdam, 1985).

Color Constancy

Color constancy is the term given to the collective effects of apparent brightness and hue constancy. Object

hue (color) tends to remain constant when the hue (spectral composition) of the source of illumination is varied over a wide range (Cornsweet, 1970), from firelight at correlated color temperatures of 1500 K, to skylight at 10,000 K and higher (MacAdam, 1985). If human vision did not possess this attribute, objects would appear different to us with every passing cloud. How then would we recognize that any given object was the same at different times? It has been established that objects reflect fixed proportions of their incident light. Thus the apparent brightness and color of an object remains approximately constant because the three receptor (R G B) ratios of various object intensities within the field of view tend to remain constant (Cornsweet, 1970).

Departures from constancy do occur when the intensities of the retinal images of objects and their backgrounds differ greatly (Land, 1959; Cornsweet, 1970). Cornsweet (1970) pointed out that the amount and direction of change in hue depends on the values from the three receptor (R G B) ratios of excitation. Thus both color and apparent brightness are fairly constant over large changes in intensity as long as the three receptor ratios of excitations between an object and its background approximate unity (ie: are proportional).

The inexactness of color constancy is evidenced by the existence of metameric materials (Evans, 1974; MacAdam, 1985). Metamers are colored stimuli (containing mixed wavelengths) that have different spectral distributions yet look alike when illuminated by daylight and exhibit color differences as the result of some other illuminant (MacAdam, 1985). It must also be noted that color constancy does not hold for some modern illuminants with low color rendering indices and if a surface is illuminated by light of a single wavelength it will reflect only the light of that wavelength (MacAdam, 1985).

Xu (1983) found that modern fluorescent illuminants have different color rendering capacities (C R C) or the color rendering properties of illumination. For an infinite number of all possible spectral-reflection types (surfaces) the total number of apparent colors would be proportional to the C R C of the illumination. In terms of color appearance, an illuminant with a high C R C would reveal a greater number of distinguishable colors than an illuminant with a low C R C.

Buchsbaum (1980) computed color constancy descriptors which are independent of ambient light flux if the average spectral reflectance of objects in the image is known. His method, however, has limited utility in remote sensing as it is unlikely that the average

spectral reflectance function of all remotely sensed object scenes can be known in advance of processing operations (Maloney and Wandell, 1986). Maloney and Wandell (1986) improved on Buchsbaum's results by estimating ambient light and surface vectors and used these estimates to recover surface reflectances permitting color correction for ambient light flux.

Gershon, Jepson and Tsotsos (1987), in an approach similar to Buchsbaum's (1980) method, computed color constant descriptors independent of illumination effects. They computed object scene reflectances out of computed color descriptors. Their two step process [1] estimating the illuminant vector and [2] using the estimated illuminant to obtain the color descriptors, was based on statistical measurements of naturally occuring reflectances and illuminants. Using spectral sensitivity curves of 370 various material types (soil, water, vegetation, etc...) they computed three characteristic vectors describing light sources (illuminants) representing the average reflectance of all materials. Their model is dependent upon knowledge of the response functions of the sensor used, limiting its utility to first generation images and carefully calibrated sensors. One might suspect that this model would also have great difficulty dealing with atmospheric effects.

The method employed by Gershon, Jepson and Tsotsos (1987) involved segmenting the image into regions first using the criteria of homogeneity. This task has been proven to be difficult under many circumstances. They suggested that the performance of their algorithm can be enhanced by restricting it to materials expected to be in the input images (eg; forests containing only leaves and wood). This is hardly the case for most, if not all, images and if it were, as with images of homogeneous forest canopy, ambient flux corrections would not be necessary for generating a satisfactory product (color map).

Brainard and Wandell, (1986) analyzed the retinex theory of color vision for its adequacy as a model of human color vision. Using a uniformly illuminated Mondrian with smoothly varying intensity changes, they applied their retinex type operator along random paths of different lengths. No thresholding operation was applied as it was deemed unnecessary because the target was uniformly illuminated. Brainard and Wandell, (1986) point out that the authors of the retinex algorithm (McCann, McKee and Taylor, 1976) failed to provide the statistical properties of the path generation process. Therefore, they chose a process which they believed simplified the analysis of dependence of the algorithm's behavior on path length. Brainard and Wandell, (1986)

noted that the contribution to (white reference point) normalization increases as the number of pixels along the path increases (eg;>200). Land (1983) inferred that the path length of his retinex algorithm must be long (Brainard and Wandell, 1986).

For this reason, a contiguous path wherein the lightness of each pixel is normalized to remote as well as near pixel values appears to be necessary. Brainard and Wandell (1986) proposed that without the updated parameters (incident angle and wavelength of ambient light and some knowledge of the reflectance and absorption functions for the type of surface imaged) offered by Buchsbaum (1980), Maloney (1985), Maloney and Wandell (1986) and Wandell (1987), any other form of retinex algorithm is likely to fail to provide color constant descriptors when the spectral power distribution of the ambient light was varied. The authors, Brainard and Wandell (1986), point out, however, that investigations by McCann et al. (1976) showed that failures of their algorithm were not dramatic and were of the same order of magnitude as human failures. The important conclusions reached by Maloney and Wandell (1986), which will be evaluated further in light of my conclusions are: [1]in the case of a long path, the dependence on the surface in the image is too strong, and, [2]the procedure did not discover a path length that

permitted the retinex algorithm to provide color constancy.

Maloney and Wandell (1986) proposed that the difficulty with the retinex algorithm is that the normalization it performs depends on different reference surfaces for different scenes and thus it is not suprising that it fails the color constancy test. Horn (1974) acknowledged this weakness in indicating the algorithm's dependence upon the existence of a white reference region. This point may also prove to be significant where specular reflectance and/or instrument noise exists in the image being processed and will be considered further in the discussion and conclusion sections.

Summary

Retinex theory accommodates all accepted aspects of established human color vision theory. Edge detection, a function performed by the hypersensitive rod cells considered important in initiating contour perception, is replicated by Land's between edge ratioing.

Brightness and hue constancy (hue constancy being the analogue of color constancy (Cornsweet, 1970)) are the underlying assumptions that Land et al.(1971;1977) have incorporated into their integrated reflectance

procedures. Both phenomena are contingent upon the relative reflectances between an object and its surrounds or background. Land's method for calculating the integrated reflectance of an object scene varied but basically involved taking the ratios of reflectances between objects and their surrounds. The result was analogous to both brightness and hue constancy.

The fact that all of the operations of the retinex correction are performed upon each individual waveband separately and then combined to generate the final color presentation can be considered analogous to the individual interactions of the red, green, and blue cone receptor sets.

Perhaps an important aspect for which current retinex type corrections have no provision is that of photoreceptor adaptation. This aspect may be critical when the sources for testing the retinex correction are the individual photographic film emulsions or electronic sensor surfaces which cannot be considered analogous to cone sets as their radiometric responses are very different and response compression performed by cones has no analogue in film or electronic sensors.

Another point of concern for remote sensing data is the underlying assumption of the retinex corrections, that illumination gradients are gradual and linear. As indicated by Marr (1982) these assumptions hold true

unless the source of illumination is very near the imaged surface. In this case gradients may be abrupt and non-linear directly under the source. Under the conditions set up in this study for testing the retinex corrections the sources of illumination were near. Therefore these and other conditions were examined in the context of the experimental results.

The reasons for selecting a computationally simple form of the retinex algorithm were; [1] Due to the diversity of surface compositions encountered in environmental remote sensing, many generalizations must be made. When we try to include all possible parameters affecting a sensor in processing images for straight forward results (eg; mapping environmental attributes) we are affected by dimishing returns. Under most circumstances the inclusion of all possible parameters is impossible. Inevitably, compromises are made no matter how many parameters are included. [2] It was difficult to believe that operations which include many generalizations for certain parameters can be significantly improved in application by the inclusion of some other highly specific parameters (eg; detailed source spectral data) when atmospheric effects cannot be determined.

III

EXPERIMENTAL METHODS

Radiometric Correction

The utility of a radiometric filtration or correction process like retinex filtration becomes apparent when one considers the limitations of multispectral sensors. For example, when the angle of incident light changes or target areas are shadowed, changes in energy flux, hue, and lightness lead to incorrect target identifications during image processing. The principal hypothesis to be tested in this study was that a retinex type correction can be used successfully to correct illumination gradients improving radiometric separation and target identification.

Many useful computational filtration processes have been developed for radiometric correction (Pavlidis, 1982). Median, low, and high pass filters are a few such procedures designed to correct for spatial and radiometric distortions associated with imagery from passive sensor systems, such as multispectral scanners. These are computational procedures which are applied to digital images. They should not be confused with photographic spectral filters which are optical in

nature. Dark body subtraction is another technique frequently used to correct for radiometric distortions caused by atmospheric effects (Chavez, 1988). This and other simple procedures are not really computational but are adjustment procedures.

Radiometric filters and procedures of the type described consist primarily of mathematical equations applied in a computerized work environment. A retinex type correction should also be suitable for such computational and adjustment procedures. Digital values can be generated for multiband photographic images as well as electronic sensor images. The digital format of any single or multiband image is based upon gray tone values similar to the separate receptor set (rods and cones) images produced by the human visual system. The discrete gray tones of an imaged scene represent both spatial and radiometric information. According to retinex theory, images are processed on a point by point basis according to gray tone (lightness) values. This type of filtration/correction is well suited to digital image processing.

Target Structure and Conditions

To test the robustness and performance of the retinex correction a suitable data set had to be established. A color target was constructed using 2.25

inch colored squares of matt-finished paper. Eight colors were used representing the six color primaries red, green, blue, cyan, magenta, and yellow plus black and white. A fully saturated cyan was not available, therefore, two disparate shades of blue were used to represent blue and cyan. The colored squares were pasted to a sheet of construction board and ordered in eight rows and nine columns.

The eight colors represented in each column were located randomly. With the colored columns configured this way, a transect along any row would result in a repeat of the colors at random intervals. An illumination condition replicating energy flux and wavelength variations causing graded illumination and hue shifts was recorded using tri-color photographic film (Kodak KR 64 5032). Graded illumination was accomplished by lighting the target from above and directly in front. By using fluorescent (GTE cool white F72T12/C.W./V.H.O.) lights overhead and tungsten directed from a frontal position, color shifts across the planar target surface would be accomplished in the resulting photographic product.

A 35mm single lens reflex camera (Asahi Pentax SP 500) fixed to a tripod and operated by cable release was used. A 55mm (Super-Takumar 1:2/55) lens with an aperture setting of f2 was employed. Light meter

readings were made using the camera's internal meter. The distance between the camera and target were dictated by the lens focal length / target size relationship. This resulted in a nominal distance of approximately 2.5 meters, permitting sufficient space for lamp positioning.

Film processing was completed under controlled conditions at the Instructional Media Centre, Simon Fraser University. As predicted, the color slide product exhibited extreme color shifts across the target image (Ped). This result produced considerable target color variability.

The three red, green, and blue sensitive emulsions of photographic film are designed to simulate the color vision sensitivities of the three cone photoreceptor sets (Fig. 1-1). Each emulsion layer responds to a broad band of frequencies. Regarding spectral sensitivity, each of the three emulsion layers can be thought of as three black and white silver halide emulsions but when viewed in composite the layers produce the visual sensation of the original scene (Lillesand and Kiefer, 1979).

Digitizing

The spectral reflectance data contained in each emulsion layer can be analyzed on a band by band basis. This was accomplished using red, green, and blue color separation filters. This resulted in three separate

images each representing the response of the individual film emulsion layer (Lillesand and Kiefer, 1979).

Kodak wratten gels (# 25, 58, and 47B) were used in video digitizing the three color separations. A TV camera (RCA Newvicon) with a macro lens adapted was used in conjunction with video digitizing software (International Imaging Systems, System 500) and the Stanford Technologies model 70 image analysis system. The input video signal representing each of the red, green, and blue bands was calibrated to a signal peak of one volt. This was accomplished using a video signal wave form monitor. This procedure ensured that the brightest point (white) recorded by each emulsion layer corresponded to the peak input video signal.

With each waveband of the target image in digital format the full range of brightness values corresponded to 256 gray tones known as DN's or digital numbers. With the 256 gray tones represented by integer values from 0 to 255 and the display format of 512 rows and columns, each band consisted of 262,144 pixels (picture elements). In relation to the retinex correction to be tested the pixels may be considered analogous to image points ready for a point by point comparison. The target conditions were represented by three separate digital images and were backed-up on magnetic tape and stored on hard disk ready for analysis.

Implementing the Algorithm

The next step in the experiment involved implementing the basic retinex algorithm in software form. A listing of the program is included in Appendix B. After experimenting for some time with small arrays and a digital calculator an approach was determined.

The between edge ratioing on a point by point basis was accomplished by comparing pixel edges in row format. Any quotient exceeding the unity value of 1.0 was set to 1.0 in order to maintain a relative scale. Any quotient values that retain the unity value upon completion of all between edge ratios served to represent the brightest points in the image scene and were thus rescaled to the maximum integer value of 255. A threshold test was also applied to all quotient pairs sharing a common neighbour to determine whether an actual edge existed due to a change in surface reflectance function or conversely, an illumination gradient.

Threshold Operator

The threshold operator was applied by taking the absolute value (ABS) between the two ratios calculated between three neighbouring pixels along a row. The middle pixel of any three pixels in a row has two common neighbours. When ratioed as illustrated (Fig. 2-1) the

absolute value of the two quotients was compared to the threshold value. Where the ABS is less than the threshold value the sequential product remained unchanged and the two adjacent pixels were considered as having the same value in the corrected array. When the ABS was greater than the threshold value a new sequential product was established indicating a change in reflectance function or an edge.

The function of the threshold was to remove gradual changes in illumination caused by light gradients and enhance edge detection. As indicated by Marr (1982) if the threshold is too low it will not serve to remove the illumination gradient and if too high valuable information may be removed.

By commencing at pixel coordinates row 1,col 1 (upper left) and proceeding in a zig zag fashion along the full length of each row to row 512,col 512 (lower right) all neighbouring pixel edges were compared as if they were of one contiguous row. Upon the completion of one pass the order was reversed and run from pixel coordinates row 512,col 512 to row 1,col 1 (Fig. 2-1). Upon completion of the second pass an array containing the sequential products of each iteration was rescaled linearly over the 256 integer range. The pixel output from each subsequent iteration represented an integrated reflectance of the entire field of view for the target

scene. This means that the lightness value of each pixel was relative to the value of the lightest pixel in the scene in terms of a percentage value (Fig. 2-1). The percentage values (1-100) provided a limited display range and were therefore rescaled to the 256 value integer format.

Direction and Iteration

The new array was saved for further iterations which were performed orthogonal to the first direction or, if satisfactory, displayed. Where further iterations were implemented the output from the first iteration was rotated using System 500 software (function 'Reorganize'). When all three wavebands had been individually processed they were merged in an additive manner and displayed as a color image.

In accounting for the somewhat unorthodox implementation of the basic algorithm, the contiguous row, the direction of implementation regarding a single pass and/or successive iterations of the program were considered factors. Iterations and direction are interrelated because changes in direction are applied to further iterations. The reason for concern regarding the direction of implementation is that some "directional preferencing" may occur propagating along a row. This, as a result of the contiguous row format of

implementation, could cause spurious radiometric artifacts.

Another consideration regarding the twin factors of direction and reiteration relates to the orientation of a pixel's adjacent neighbours. Depending upon where in a scene a pixel is located its number of adjacent neighbours changes. As can be seen in (Fig. 3-2) pixels which constitute image edges may have as few as three and as many as five adjacent neighbours, whereas pixels located well within image boundaries will be associated with eight common neighbours but only half are subjected to direct comparison. This results from the fact that the algorithm does not run diagonally.

Whereas direction and reiterations are interrelated another possible factor must be considered. In the first pass of the algorithm each pixel was compared in row format to two of its four (row and column) neighbouring pixels. Upon reiteration incorporating a new direction each pixel was compared in column format to its two remaining (row and column) neighbours. Thus each pixel was compared with an increasing number of its neighbours (Fig. 3-2).

Threshold Value Selection

Another factor considered was the selection of appropriate threshold values. Horn (1974), Marr (1982),

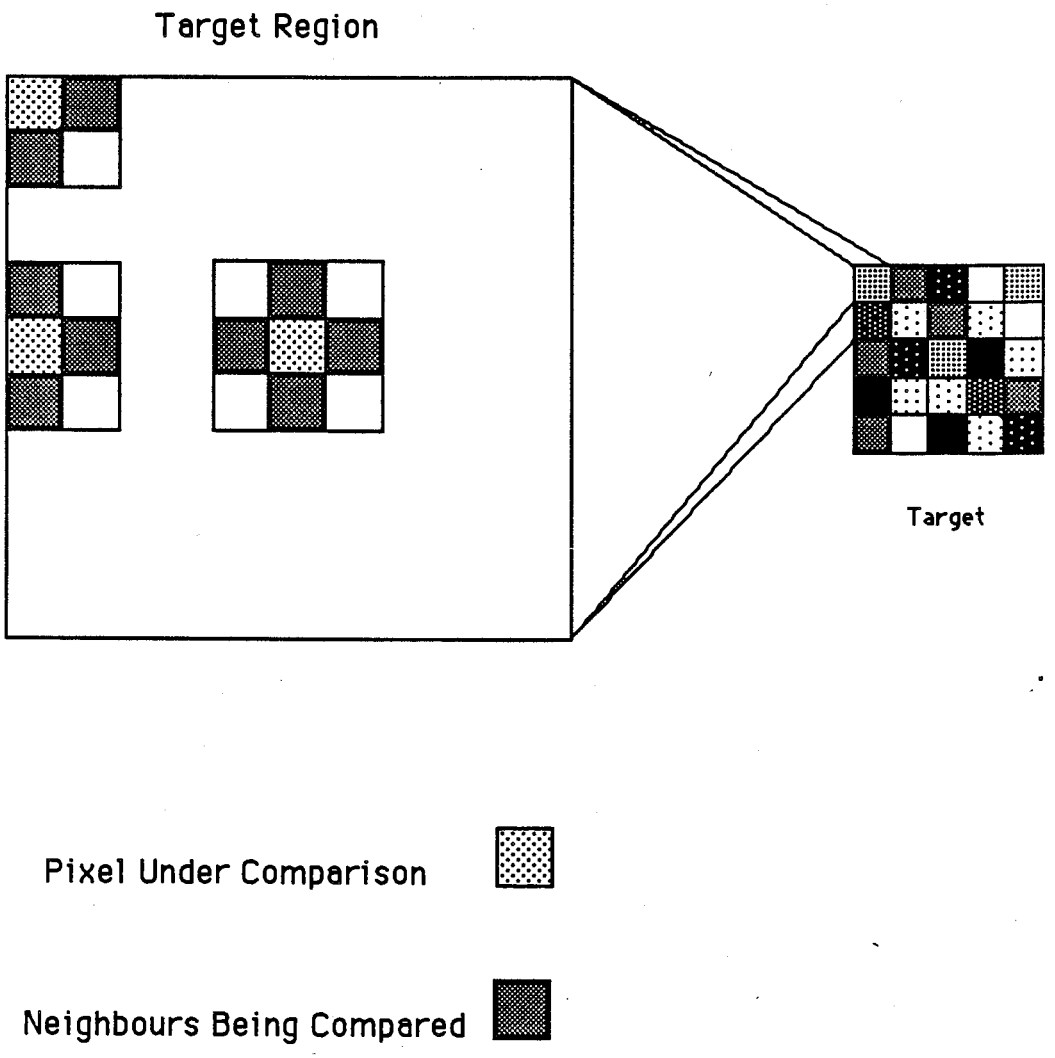

Fig. 3-2. Diagram indicating which neighbours are compared after one reiteration (2 directions).

and Terzopoulos (1986) have each addressed this consideration in the context of their choice of implementation. Each concluded that selected values must perform the function of eliminating gradual changes representing graded illumination while maintaining edge detection continuity.

This conclusion provides no obvious insight regarding threshold selections as they pertain to this experiment. The range of integer values representing the digital image does, however, provide some guidance toward suitable threshold selection.

Let us consider for instance that an incremental or decremental difference of one DN represents change caused by graded light but a difference of two DN's defines an edge; then the choice is simple. This is, however, rarely the case. Upon video digitizing, a resulting gray tone image is represented by as few as 65 DN's (0-64). Due to spherical and chromatic aberations often associated with manufactured lenses (Cornsweet, 1970), the range of target brightness values is not uniformly represented by equal intervals of the DN range. For instance target areas which are black may not be represented by DN's ranging from 0-7 as white areas may not be represented by the DN range 56-64 with the intermediate gray tone values equally distributed.

Within any given target area the range of DN's can exceed the difference across an actual edge. In other words, enclosed within a gray tone area represented by a DN range from ten to twenty may exist an anolomonous DN with the value of twenty-five and/or seven, etc. This anomolous DN may be within the range of an adjacent area. When encountered by the threshold operator the anomoly will mistakenly be defined as an edge.

The actual DN's of any two different gray tone areas can be represented by DN's with a minimum integer value of 10 and a maximum value of 30. Such would be the case where intensities were not uniform also where increases or decreases in intensity were also not uniform. With the edge between the two separated by a DN difference of 2 and the range unevenly distributed in each of the two areas, which set of all possible differences will the threshold value best represent?

Once a threshold value is assigned (0.004) its influence is proportionately greater upon high DN values than low DN values. Ratios between high integer values will produce smaller real numbers than ratios between lower integers, even when the DN difference is the same between the values being ratioed (Fig. 3-3). This results in the threshold having an effect which is potentially five times greater upon areas represented by DN's of high integer value.

Low and High Integer Ratios

8 / 10 = .8

10 / 12 = .83

ABS (0.03)

26 / 28 = .9286

28 / 30 = .933·

ABS (0.005)

58 / 60 = .966·

60 / 62 = .9677

ABS (0.001)

201 / 203 = .99015

203 / 205 = .99024

ABS (0.00009)

Figure 3-3. Hypothetical DN values represent how different integer ranges are affected by a set threshold operator where DN's are separated by a DN difference of 2.

A means of diminishing this effect can be achieved by pedestalling the DN range. This technique raises each value in the array by an equal amount. Although all DN values are increased, resulting in an overall brighter image, the relative differences between the DN's remains unchanged. This will minimize the differential effect of thresholds upon ratios. For instance, within the integer range 191-255 all ratios will fall within the same order of magnitude when the DN difference is the same (Fig. 3-3). This gives the thresholding process greater uniformity of effect.

Given these factors, it becomes clear that the selection of a threshold value is contingent upon the effects of pedestalling. A major consideration of these experiments was, therefore, testing the algorithm with different combinations of thresholds and pedestals. This, in addition to the effects of iterations and direction, constituted the bulk of the experimental data.

Land (1977), using data of integer values within the range of these data, suggested using a threshold value of 0.003 for the ratio threshold in testing whether two adjacent points varied sufficiently from unity to be considered different. Marr (1982), suggested that a threshold operator must be high enough to remove differences caused by graded light without removing valuable information from shaded areas. Given the

integer range of the experimental data and the consideration that using as high a threshold operator as possible without deleterious effect, the threshold value 0.004 was chosen as the primary value for testing. The ratio threshold mentioned herein is the only thresholding operation under consideration. Other threshold operations could be applied at different stages during calculations, however, no provision to do so has, as yet, been included in the software.

Included in Tables 1 through 4 are 14 runs of the program applying the basic algorithm. The individual runs were selected to determine the effects of varying the threshold, iterations, directions, and pedestal parameters. Table 1 indicates which runs were included in varying threshold, iterations, and directions while holding the pedestal value constant. Here the pedestal value was set to a minimum value of one to avoid arithmetic errors caused by dividing by zero. In this sub-set direction and iterations were interrelated by the fact that iterations were performed after successive rotations each at 90^0 in a clockwise direction. This method of rotation resulted in the algorithm using a different departure point for each iteration.

Table 2 contains runs within which thresholds and iterations were varied while holding direction and pedestal values constant. Here the pedestal values were

set to a mean value of 128 for each of the three wavebands (facilitated by using a system 500 program adjust). In doing so the standard deviation of each waveband was maintained, resulting in no other transformation than centering around a common mean. Direction was held constant by flipping the image back and forth about its geometric axes (Fig. 3-4) defined by its origin (1,1) and extreme (512,512). (This was accomplished using system 500 program transform).

Table 3 contains runs wherein all four parameters were varied. In Run 23 the threshold was increased upon reiteration to test the effect of this procedure. In run twenty-four thresholds were varied for each separate waveband (Red= 0.0046038; Green= 0.004'; Blue= 0.0046729). Individual image arithmetic means from white regions within each waveband served as the pedestal references for this test. These values were extracted using the system 500 (blotch and statistics) programs. Upon defining an area representing a region of white on the color target by enclosing it in a polygon, image statistics can be printed for that area. Arithmetic means were determined using this method for each waveband's mean white value, ratioed by a +/-1 DN difference, threshold values close to the value 0.004 were selected. In this case, the terms for threshold

Fig. 3-4. System 500 rotation functions used in implementing direction changes for reiteration.

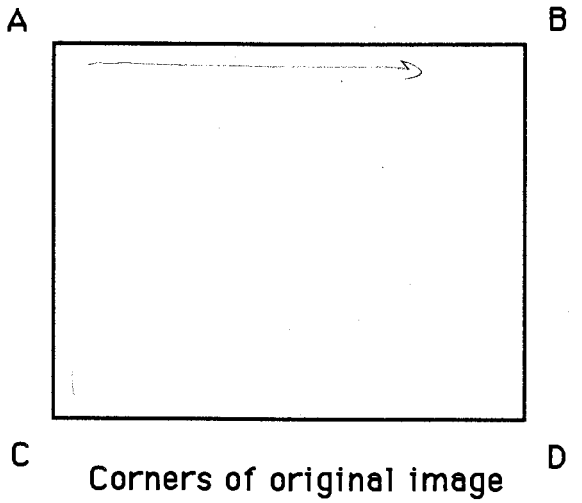

Corners of original image

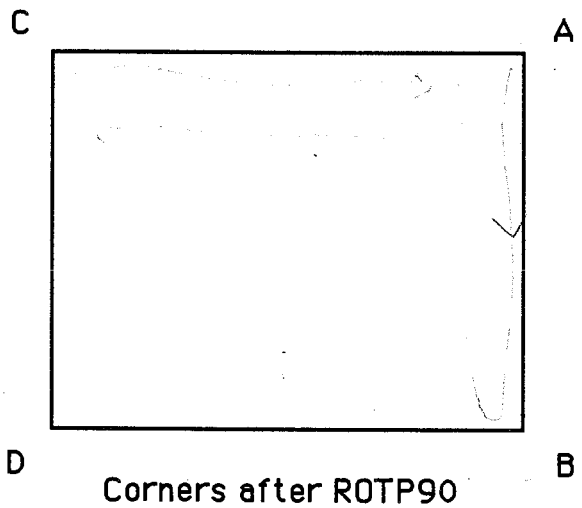

Corners after ROTP90

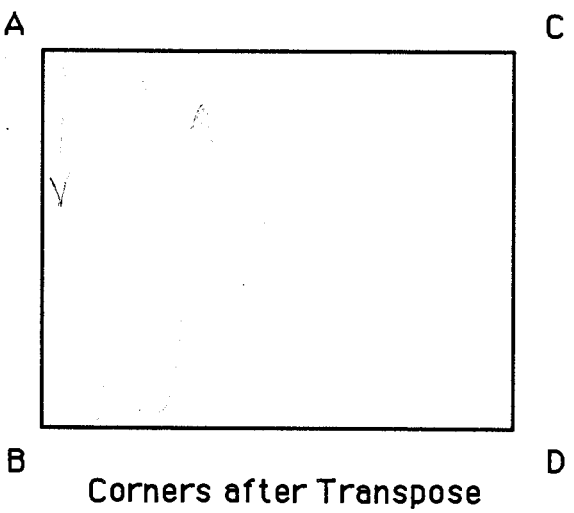

Corners after Transpose

selections were somewhat arbitrarily chosen for the sake of experimentation.

Table 4 contains runs wherein all values other than the pedestal value were varied. The selected peak white pedestal value here was the maximum value of 255. This means that the brightest value in each waveband was pedestalled to 255 to increase the range of integers to which the threshold operator would apply (Fig. 3-5). As in Tables 2 and 3, changes in direction were accomplished using System 500. Thresholds have been varied by waveband and in one instance, run thirty-one, the threshold value was increased slightly upon reiteration.

Analyses

The preceeding factors and their associated results were analyzed in sequence. The principal hypothesis was that this correction can successfully be used to approximate a condition of even illumination increasing the reliability of target identification and radiometric separation. Examination was accomplished using the system 500 image analysis system in conjunction with a color graphics recorder (Matrix Camera).

Upon the completion of each run, a photographic copy of the corrected color scene was qualitatively compared for color rendition and general appearance. If successful in approximating a condition of even

Fig. 3-5. Image profiles of the same image with and without pedestal in place. Pedestal value (constant) serves to increase the effective range of the threshold operator.

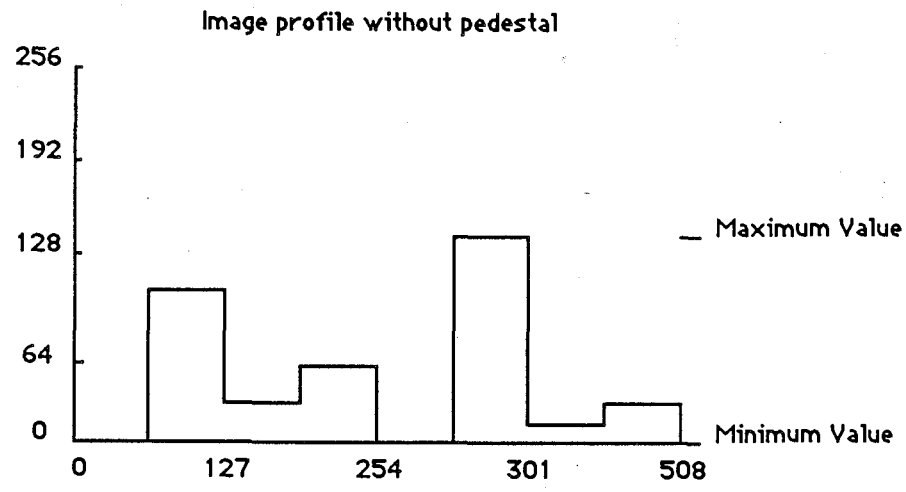

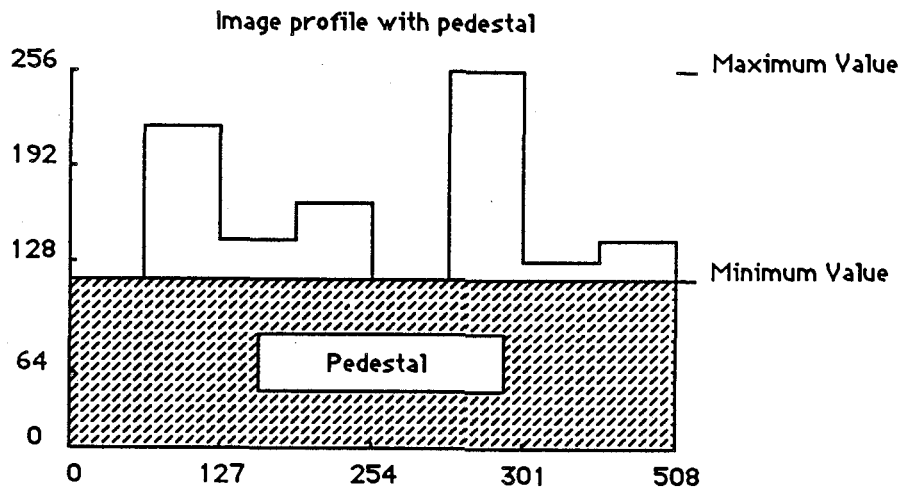

illumination an increase in correct target classification by color would be evident. Hue and brightness constancy if inherent to the correction, would also be manifest in a satisfactory color rendition.

The property of edge detection as outlined in the theoretical section should be explicit in the photographic product. In testing the premise that improved radiometric separation will result from the correction image data profiles and histograms were examined. Profiles were restricted to a single column centrally located encountering all eight primary colors. Assuming that the correction worked as predicted, profiles should demonstrate a presence of the retinex effect (Fig. 3-6) (reduction of graded illumination and edge enhancement).

Profiles should also indicate the presence and reduction in relative noise levels. The differential effects upon the three different wavebands should be evident when plotted in profile. Changes in DN ranges were also examined by data profiles.

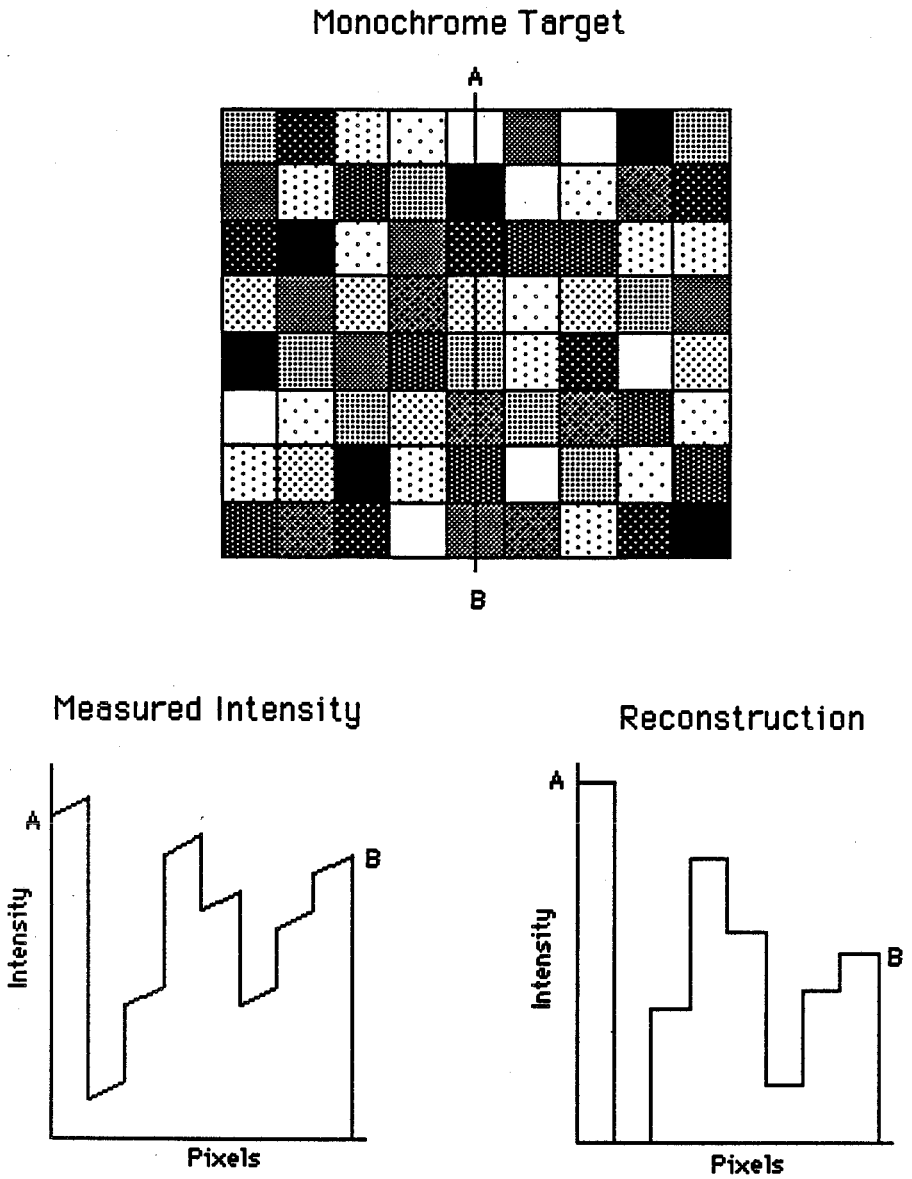

Fig. 3-6. Diagrams illustrating top to bottom profile of monochromatic target (ie. blue band) with illumination gradient. Profile plot of line A B by measured intensity. Profile plot after reconstruction indicating " retinex " effect.

IV

EXPERIMENTAL RESULTS

Effects of Direction and Reiterations

Tables 1 through 4 list different runs of the algorithm where the input data are represented by a compressed range of integer values DN^S (1-127). The input images to be corrected for graded illumination are referred to herein as Ped (pedestalled by minimum value 1); Hiped (pedestalled by mean value 128); and Est'ped (pedestalled by maximum value 255). Resulting photographic products including images, profiles, and histograms are contained in Appendix A.

An objective assessment of the influence of directional differences alone is difficult. Direction may be spuriously correlated to reiteration. As previously mentioned, changes in direction with successive iterations are required if pixel normalization is to include orthogonally adjacent neighbours. Changes in direction are also implemented to counterbalance possible effects of directional preferencing.

Directional preferencing is manifest in the form of the striping artifacts clearly visible in runs incorporating too high a threshold value (run 17, run 19, run 23, and run 24). A color plate of run twenty-four

indicates that striping artifacts were not simply a function of reiteration as they appeared with one pass in the initial direction where threshold values were unsuitably high (Table 3).

Reiterations were performed upon all three classes (Ped, Hiped, and Est'Ped) of the target image. Ped class images were manipulated for reiteration using the System 500 program Reorganize (Rotp90). Upon the completion of one pass of the algorithm the output arrays were rotated ninety degrees in a clockwise direction before reiteration. A full three hundred and sixty degree rotation of the image resulted in five iterations with each successive iteration beginning at different departure point pixel coordinates. Reiterations performed upon Hiped and Est'Ped image classes were facilitated using the program Reorganize (Transpose). While changing direction of successive iterations this effectively increased the path length during execution by using the same departure point pixel coordinates for each following iteration.

The most immediately reconizable and deleterious result of multiple reiterations (runs one, five; six, ten; and twenty-one, twenty-eight) was the increase in radiometric noise particularly within the brightly illuminated areas. Profiles of runs five, ten, and twenty-eight clearly portray poor signal to noise ratios

across target regions resulting from multiple reiterations. Examination of color plates of these three runs clearly indicated, however, the edge definition effect associated with this parameter.

Another positive effect of multiple reiterations was the extraction and definition of information from shaded regions. Examination of the color plates of the above mentioned runs clearly demonstrated this. Color plates of runs twenty-seven and twenty-eight indicated the presence of additional pixel class assignments in the upper left (dimly illuminated) region of the target with the added iteration. This evidence indicated that multiple iterations are necessary for improving the feature extraction performance of the algorithm. Some means of suppressing noise, however, must be employed to improve signal to noise ratios.

Path Length

Profiles of the image classes Hiped and Est'Ped subjected to only one reiteration (no increase in threshold) of the algorithm are included for runs twenty / twenty-one and twenty-nine / thirty respectively and show no appreciable difference when compared to the same image with one pass of the algorithm. One might conclude therefore that the path length traversed by one pass of

the algorithm (524288 pixels) was sufficiently long to achieve white reference point normalization.

Effects of Pedestals

Pedestals have been employed for two reasons. First they avoid the arithmetic errors (log of zero and divide by zero) encountered in image classification. Second they increase the range of integers to which a threshold value would apply. Runs one (Ped) and twenty-nine (Est'Ped) represent the two extremes of the three image classes employing the same threshold value and no reiterations. Image profiles of these runs indicated that, after processing, the highly pedestalled image shows an improved retinex effect and less noise when compared to its counterpart run one. It may be concluded that these effects resulted from the range compression response produced by the algorithm.

Runs twenty-one (Hiped) and thirty (Est'Ped) employed the same threshold value and one reiteration each. These two images represented smaller compression responses upon processing than are presented between the two extremes Ped and Est'Ped. This difference is presumably due, somehow, to pedestalling. Radiometric slopes measured from image profiles of runs twenty-one and thirty within the yellow region (red band) between profile pixel coordinates X=42 and X=108 indicated no

change between the two different runs. A marked reduction in slope may be interpreted as having resulted from the retinex effect (removal of illumination gradient).

When compared to the unprocessed images Ped and Hiped, run one and twenty-one, in fact, appear to have produced an increase in gradient for this same region. The increased slope after processing in runs one and twenty-one is believed to have been generated by the linear stretch employed by the program after normalization. It may be safely concluded, therefore, that no significant change in the algorithm's performance resulted from pedestalling other than increasing the effective range of the threshold value. This factor alone should result in some improvement in illumination gradient smoothing.

Threshold Selection

As outlined in Chapter Two, the threshold operator was designed to remove small linear changes in illumination caused by light gradients. Selected threshold values ranged from very fine (0.00004) to very coarse (0.010). Threshold selection was enigmatic. Thresholds have been applied to integer ratios by first taking the absolute values (ABS) of the ratios of two adjacent pixels. If that ABS was equal to or exceeded

the predefined threshold value a change in surface reflectance was assumed and the resulting ratio value represented this change. If, however, the ABS of the ratioed pixel pair was less than the threshold value no change in surface reflectance was assumed and the pixel was assigned the value of its last immediate neighbour. This is based on the assumption that gradual differences are presumed to have resulted from graded illumination. The results in this case are pixel neighbours with the same uniform values. Hence upon completion of the process only changes due to surface reflectance function and not graded light, ultimately, are preserved.

During early experiments with this program threshold values were selected arbitrarily in order to gain insight to the effects of value selection. Where images were represented by integers of a somewhat compressed range (0-127) extremely fine thresholds had no effect upon ABS values of smaller DN (1-32) ratios. For instance, if the effect of graded light is assumed to be small (+/- 1 or 2 DN^S) then one is forced to assume that some DN value greater than this represents the radiometric target change to be identified. Take for instance three adjacent pixels of DN values 10/12/14. The ABS value of their resulting ratios would be ((10/12 and 12/14) ABS = 0.0238095). Three adjacent pixels of DN values 58/60/62 have resulting ratios((58/60 and 60/62) ABS = 0.001)

yielding an absolute value of a different order of magnitude.

It is immediately evident that any threshold value implemented in this manner will serve its designed purpose upon only a limited range of DN values. The fact that each separate waveband has its own characteristic response to a color stimulus further complicated threshold selection. A blue target area (color stimulus) is represented by gray tone DN values which are highest in the blue band, lower in the green band and lowest in the red band. The same type of variation can be observed for all other color stimuli with values, depending upon the initial target properties. The difficulty encountered was in selecting a threshold value that would perform equally well for all color stimuli. Assuming that a suitable threshold value can be selected for gradient removal within a particular wave band, will that threshold be suitable for all three radiometric bands?

Runs twenty-one and nineteen represented threshold values (0.004 0.005) differing by 0.001, each having been subjected to one reiteration (common origin). Runs one and six represented one pass (no reiterations) of the algorithm, wherein the threshold values (0.004 0.006) used for the two tests differed by 0.002. Runs five and ten were similarly separated by threshold value but

involved multiple iterations (same threshold) wherein each consecutive iteration was initiated from different starting point coordinates. Reiterations performed upon runs included in Tables 2 through 4 were initiated from the same starting point coordinates, resulting in an increased path length of common origin.

Profiles, taken along the same central column of these images, indicated a noticeable difference between runs twenty-one and nineteen. No change was evident between runs one and six, while the differences between runs five and ten were again conspicuous.

Although noisier than their counterparts without multiple reiterations, the higher threshold used for runs five and ten had an interesting two part effect. First, the higher threshold employed with run ten compressed the overall integer range. This result was expected as higher thresholds eliminated intermediate DN values associated with small DN increments induced by graded light. Second, the compression effects appeared to be somewhat band specific.

Differences in range compression also appeared to be band specific for Hiped images runs twenty-one and nineteen. Range compression within the blue band appeared to be less pronounced than it is for the red and green bands between the two runs. Image statistics for these profiles have been included. The standard

deviation for each run indicates that dispersion, after processing, is consistant with findings from profile plots for each wave band.

Increases in radiometric slope for the white target area can be seen in run nineteen (green band) and run ten (blue band). This increase centered at pixel 378 along the profile line was associated with striping artifacts.

Profiles of runs twenty (0.004) / twenty-three (0.005) and twenty-nine (0.004) / thirty-one (0.00425) represented changes in the input images Hiped and Est'ped when the threshold value was increased by 0.001 and 0.00025 respectively between iterations. Again these results indicated band specific (red and green band) range compression with a marked depression of values in both bands upon reiteration. Run twenty-three also contained striping artifacts as a result of threshold increase. Predictably, run thirty-one also exhibited an increase in noise in all bands as a function of reiteration.

Striping artifacts resulting from using too high a threshold value (0.010) were evident in the color plate of run seventeen. A radiometric image profile of this run shows the badly distorted output. Conversely, in order to test the effect of a very low threshold value (0.00004), run thirty-nine was made. This run included one reiteration using the same threshold value. As

expected, a profile of this run indicated little change from the original Est'ped. No significant range compression or depression was evident while the signal to noise ratio had not noticeably changed. A slight indication of the retinex effect was evident in the yellow and red target areas of the red band. This may further suggest a need for band specific thresholding. Image histograms for the tabled runs indicate that the algorithm performs a noticeable smoothing operation in all cases. The range compression effect of the algorithm, however, has resulted in very flat histogram plots.

Salient Features

To limit the results for this experiment to the evaluation of statistics, profile plots, and histograms would overlook an important aspect of interpretation. As no means of exacting changes in hue, luminosity, and saturation in a controlled manner was available for these photographic products, a qualitative analysis was included. As noted in Chapter Two, of the three variables, hue is the quantity of some color and is the variable which changes most strongly with shifts in wavelength. Luminosity or the quantity of light, changes with intensity while saturation, the whiteishness of the color changes with the purity of the hue.

When juxtaposed with the image Ped, runs one and six show a marked improvement in picture quality. With processing, some of the illumination gradient had been displaced. Colors exhibited a marked increase in luminosity as a result of white region normalization and linear stretching. No changes in wavelength which might affect hue resulted from this type of processing; however, the purity of the hues where the illumination gradient had been displaced produced richly saturated colors. This was most strongly evidenced by the yellow regions in columns six and seven. Again, this appeared to have resulted from white region normalization in combination with an effective threshold value for the integer range encompassing these regions.

Contrast between regions was also substantially improved, resulting from enhanced edge definition in combination with the sustained saturation. Although some improvement in contrast resulted merely from pedestalling, saturation in these instances was sacrificed.

In comparing the Hiped class of images, run twenty-one was juxtaposed with its unprocessed parent image. Immediately evident was the overall brightness of the image resulting from the pedestalling process. As might have been predicted, color saturation was severely sacrificed with this process. The higher the pedestal

the greater the desaturation. After processing, contrast was enhanced throughout run twenty-one by improved edge definition. This was most noticeable between the cyan and green regions of columns four and five of row five where in the parent image Hiped edge blurring is clearly evident.

When compared to their unprocessed parent images (Est'Ped), runs twenty-nine and thirty-nine exhibited equally interesting results. Although image profiles of these two runs indicated slight differences (eg; run thirty-nine exhibits a better retinex effect for the yellow region in column five of the red band) the color plates appeared very similar by visual comparison. A slight difference in color saturation existed between the two plates.

Little if any improvement in contrast through edge definition has resulted from run thirty-nine because of the limited range affected by the very low threshold value (0.00004). Range effect in this instance would primarily have been within the limits of the yellow region of the red and green bands and white regions of all three bands, because of the high integer values representing these regions. This range may have also included colors represented by high integer values within their respective bands (eg; some magenta and red regions in the red band, etc).

Run twenty-nine exhibited an improvement in contrast by improved edge definition compared to its unprocessed parent image and run thirty-nine. Color appeared less desaturated than in run thirty nine. However, these two photographic plates were processed in two separate batches which may have affected this result.

Summary

In summary, the results obtained by comparison with the unprocessed arrays, when varying threshold values, were as follows. Higher threshold values suppressed the effects of noise caused by multiple reiterations of the algorithm. Where threshold values were restricted in effect to the median and higher range DN values, saturation was preserved with increases in luminosity, both of which enhanced contrast. Higher threshold values limited by range to the eight bit end of image DN^S did not noticeably improve contrast, nor did they enhance saturation.

Compression of the overall integer range, accompanied by a marked depression of DN values where higher thresholds were reiterated, appeared to be band specific. Increases in profile slopes resulted from: $_A$. use of too high threshold values, manifested in the form of striping artifacts which severely degraded the images, and; $_B$. integer range stretches performed by the linear

stretch used in the program employed in processing (Rtex1_Threshold). The signal to noise ratio was not sacrificed with reiteration where higher thresholds (within limits) were maintained or increased between successive runs. Very low threshold values applied to the highly pedestalled arrays resulted in only negligible changes overall but did result in some band specific (red band) retinex effects. These results indicated that better overall results may be obtained by applying range specific threshold values on a band specific basis and increasing threshold values slightly between successive iterations.

Multiple reiterations of the algorithm were necessary for good edge definition. Unfortunately, however, isolated "salt and pepper" noise accompanied this performance. This too may be overcome by increasing (within limits) threshold values between reiterations. Multiple reiterations also resulted in information extraction from heavily shaded regions. No significant difference accompanied one reiteration of the algorithm which suggesed that multiple reiterations accompanied by some means of noise suppression would result in an improved performance.

V

DISCUSSION

In recent years a revived interest in human color vision has produced much valuable information for image processing. In many cases the objectives of the researchers involved have been oriented toward applications in artificial intelligence and not remote sensing specifically. Nevertheless, many contributions have provided improved performance of retinex type corrections. Among these contributions are those of Horn (1974); Burns, Smith, Pokorny, and Elsner (1982); Stiehl, McCann, and Savoy (1983); Maloney (1985); Gershon, Jepson, and Tsotsos (1987); Ho and Funt (1988); Funt and Drew (1988).

Applications specific to remote sensing needs have yet to be addressed by many newly developed techniques, however, these are certainly forthcoming.

An assessment of this technique would not be complete without being tested under actual remote sensing conditions. Included in this section is a brief description of the algorithm's performance under conditions commonly encountered in environmental remote sensing.

In ascertaining the utility of the algorithm used herein post analysis processing included applying the software to four Landsat images of a region in northern

Manitoba. The four images were subjected to a conventional dark body subtraction technique and white region normalization. One image in particular, a 1973 MSS image, provided a robust test of the algorithm's performance. Atmospheric scatter at the time of data aquisition for the 1973 image was severe, resulting in considerable image degradation.

Comparison of atmospheric correction performance for the two separate techniques indicates that the retinex type correction shows a substantial improvement over the alternative. Improvements consistant with the experimental results of this project were clearly evident. These include enhanced contrast and signal definition. Also included in the output product was a considerable improvement in edge definition which could of course not be expected from dark object subtraction. As a result of the edge definition performance of the algorithm, linear features (eg; roads, shorelines, and water sediment load boundaries) were substantially enhanced. As might be expected, images containing striping artifacts, as a result of sensor noise, would be similarly affected.

The presence of clouds and/or electronic noise in an image may inhibit the performance of white region normalization. In the case of the former, clouds at the top of the atmosphere would provide a white region

unrelated to surface reflectance, resulting in image normalization to an erroneous bench mark. Similar results may occur in the presence of electronic noise.

Although the hypothesis that these results demonstrate an atmospheric correction remains unsubstantiated, the overall appearance of the two sets of images for interpretation purposes indicated comparably better performance on the part of the retinex type process. Continued experimentation with this algorithm is clearly necessary before a conclusive decision regarding performance can be made.

CONCLUSIONS

The results obtained from this experiment indicate that the between edge ratio technique with white region normalization as implemented herein does not provide color constancy descriptors for the target conditions encountered. Within limits, however, a condition of even illumination has been approximated leading to a marked improvement in image quality. Conclusions were presented with attention to each of the relevant parameters examined.

The main consideration regarding direction of implementation was the comparison of all orthogonal pixel neighbours. Directional changes between successive iterations are necessary for this reason. The rotation

technique (Transpose) employed in facilitating directional changes for the Hiped and Est'Ped class images considerably reduced processing time between iterations in comparison with the software used for the Ped class images. As this is desirable it should be employed with all future applications of this program.

Under conditions involving the use of too coarse a threshold, error propogation in the form of directional preferencing produced striping artifacts. Since no other noticeable directional errors were evident it may be concluded that selection of a suitable threshold would avoid this type of error.

Multiple reiterations appear to be necessary for information extraction from severely shaded regions but must be accompanied by some means of noise suppression. Further experimentation regarding the fine tuning of thresholds between successive iterations is required and would likely produce insight for improving the technique for future implementation.

Multiple iterations also provided noticeable improvement in edge definition between regions in a manner reminiscent of human visual perception. Intensity distributions akin to those produced by Mach bands, have resulted between gray tone regions within each waveband. This is evidenced in color plates of runs five and twenty-eight where the additive effect of the color

display has produced brighter strips between regions. It was suspected that this resulted from some contribution of " point spread function ", a distortion associated with video digitizing. Further investigation regarding the persistance of this effect with reiteration will be necessary before any conclusions may be made.

The use of pedestals in association with threshold selection leads to ambiguous conclusions. While serving as a means of expanding effective threshold range, certain problems are commensurate with their utility. One such problem is what is to be done with the pedestal value remaining after processing? If pedestals are to be utilized some method of rescaling must be devised to accompany them. This would further complicate the processing and is not the most desirable solution.

An alternative to pedestalling might employ a more localized approach to threshold value selection. With such an approach threshold values might be selected and applied upon determining local variations in light gradient for finite integer ranges. Such an approach would still be limited to small, near linear illumination gradients but would stand a better chance of overcoming the confinements of such ranges.

Where illumination gradients are small and near linear, a suitable threshold value can be selected for the appropriate bit range of an image. Therefore,

assuming that the proper sequential order for applying threshold values can be assessed by some means, values either coarse or fine could be applied, having effects of the same order of magnitude for each integer range.

Results thus far have indicated that threshold values affecting median and higher range values of seven bit images (128) preserve saturation while improving contrast, whereas thresholds limited by range to the eight bit (256) end of images do not noticeably improve contrast or enhance saturation. One might conclude therefore that these results contain reasonably good evidence for range specific thresholding.

Horn (1974) found that applying the retinex operation to an image considerably reduced the range of values because the output was more closely related to reflectance. He points out that the output range will be limited to one or two orders of magnitude while the input range differs in order of magnitude because of the effect of illumination gradient. Hence, it would appear that one might safely conclude that the algorithm is performing with some degree of success.

Color plates clearly indicate that color constancy has not resulted with processing. This is no doubt partially due to the lack of spectral range overlap of the photographic filters (Wratten # 25, 58, and 47B) used when video digitizing in approximating the spectral

sensitivities of human photo receptors. Under such restrictive conditions a proper assessment of the relative degree of excitation is severely inhibited.

Photographic film, though designed to approximate the spectral sensitivities of human photoreceptors has at best only a poor similarity. Film emulsions do not respond to light stimuli with the response compression that the red, green, and blue photoreceptors of the retina do. This inability on the part of photographic film does not permit the same relative degree of excitation to be recorded by each waveband. Hence the resulting brightness values upon digitizing are not readily comparable by relative degree. Horn (1974) reported similar findings based upon recording sensitivity. He noted that if the sensors are not equally sensitive outputs will be offset. It stands therefore that some adjustment by waveband for gain is necessary for a fair assessment of the algorithm's abiltiy to provide color constancy.

It may be that the target conditions used in this experiment have simply exceeded the limits of the algorithm's performance abilities. The close proximity of the illumination source has generated nonlinear grading of illumination within some target regions and also resulted in specular reflectance directly beneath the light source. These conditions have produced effects

which would limit any linear correction. Even with the more promising techniques which claim color constancy computation utilizing linear models, illumination is assumed to vary slowly (Funt and Ho, 1988).

I have included for comparison color plates of the image Ped subjected to standard normalization and linear stretch. Both of these transformations have severe difficulty in overcoming the nonlinear effects generated by the target conditions. The retinex type of white region normalization and linear scaling has by comparison obvious advantages over either of these alternatives given the severity of illumination conditions.

Table 1. Thresholds, Iterations, Directions and Pedestal

Run #	Threshold	Reiterations	Directions	Pedestal
1	.004	None	1	Min. 1
5	.004	4	5	Min. 1
6	.006	None	1	Min. 1
10	.006	4	5	Min. 1

Table 2. Thresholds, Iterations, Directions and Pedestal

Run #	Threshold	Reiterations	Directions	Pedestal
20	.004	None	1	Mean 128
21	.004	1	2	Mean 128
28	.004	6	2	Mean 128
19	.005	1	2	Mean 128
17	.010	1	2	Mean 128

Table 3. Thresholds, Iterations, Directions and Pedestal

Run #	Threshold	Reiterations	Directions	Pedestal Value
23	.004/.005	1	2	Mean 128
	.005			
	.005			
24	.0046083	None	1	Mean 216
	.0044444			224
	.0046729			213

Table 4. Thresholds, Iterations, Directions and Pedestal

Run #	Threshold	Reiterations	Directions	Pedestal Value
39	.00004	1	2	Max. 255
	.00004			
	.00004			
29	.004	None	1	Max. 255
30	.004	1	2	Max. 255
31	.004/.00425	1	2	Max. 255

Table 5. Profile Statistics

Run #		Red	Green	Blue
1	Mean	103.728	80.324	94.610
	Std. Dev.	83.175	75.455	47.556
5	Mean	88.047	76.190	87.045
	Std. Dev.	72.578	74.809	48.281
6	Mean	103.929	80.40	93.642
	Std. Dev.	83.134	75.510	47.597
10	Mean	74.489	51.848	55.398
	Std. Dev.	62.274	51.047	38.650
20	Mean	165.379	156.874	161.685
	Std. Dev.	49.358	42.328	27.735
21	Mean	164.379	155.919	160.771
	Std. Dev.	49.358	42.294	27.636
28	Mean	122.438	148.549	154.839
	Std. Dev.	63.725	62.532	63.487
19	Mean	96.950	123.179	148.706
	Std. Dev.	28.382	50.405	25.706
17	Mean	108.001	46.679	49.356
	Std. Dev.	41.016	46.697	18.608
23	Mean	147.573	119.487	153.465
	Std. Dev.	44.231	32.343	26.319
24	Mean	159.708	133.854	128.850
	Std. Dev.	48.400	36.961	22.807

39	Mean	178.293	167.582	174.107
	Std. Dev.	41.952	37.426	24.356
29	Mean	179.104	168.132	174.899
	Std. Dev.	41.555	37.589	23.915
30	Mean	178.003	165.781	174.822
	Std. Dev.	41.576	37.138	23.920
31	Mean	144.548	157.524	174.964
	Std. Dev.	34.120	36.123	24.819

Glossary of Terms

Bit: Binary digit.

Brightness: The quality of radiating or reflecting much light (MacMillan Contemporary Dictionary, 1979). The attribute of visual perception in accordance with which an area appears to emit more or less light (Manual of Remote Sensing, 1983).

Dark Object Subtraction: A method of removing the effects of atmosphere from airborne or orbital remotely sensed images by subtracting from the overall image values any numeric amount found within the enclosed area of an object assumed to have the response of a blackbody. A blackbody is assumed to absorb all incident energy.

Directional Preferencing: The propagation of erronious results in one direction associated with the processing of digital arrays.

Edge: Intensity changes as a function of surface reflectance, not confined within the limits of illumination changes.

Electromagnetic Energy Flux: Changes in the rate of flow of light energy through a given area or medium.

Gain: A general term used to denote an increase in signal power in transmission from one point to another (Manual of Remote Sensing, 1983).

Integrated Reflectance: The bringing (parts) together into a whole. Reflectance: ratio of radiant energy reflected from a surface to the total energy falling on a surface (MacMillan Contemporary Dictionary, 1979).

Lightness: The quality or state of being light; brightness (MacMillan Contemporary Dictionary, 1979).

Mach Bands: After Ernst Mach, (1865) areas that are identical in intensity can differ in brightness. When two uniform strips differing slightly in intensity are juxtaposed the boundary between them appears nonuniformly enhanced.

Mondrian: A type of target used by Edwin Land in his experiments on retinex theory. Land named the target after the painter Piet Mondrian. The target consists of an array of rectangular overlapping shapes of gray tones or colors.

Offset: To balance or compensate for in terms of calibrating sensor data to a common mathematic intercept.

Point Spread Function: A distortion associated with video digitizing which reflects how different points contribute to the value of a sample depending on their distance from it.

Radiometric Filtration: The removal of certain spectral or spatial frequencies associated with gain and offset variations of sensors which collect radiation data, resulting in improved image features.

Appendix A

Parent Images

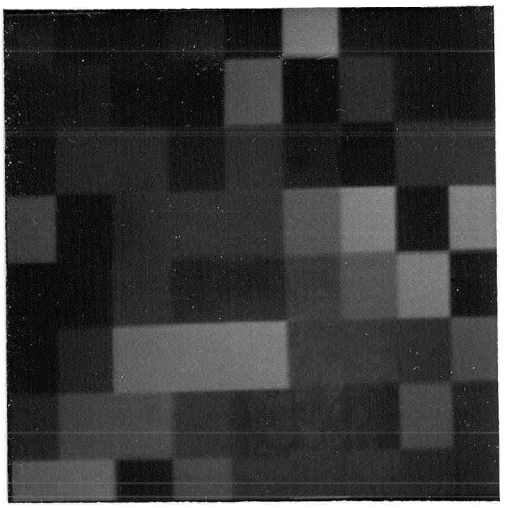

PED

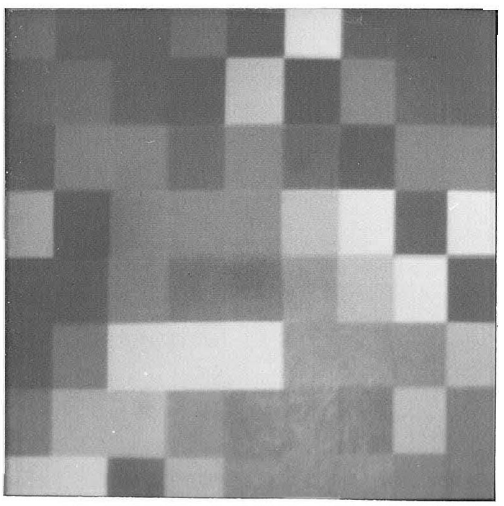

HIPED

Appendix A

Parent Images

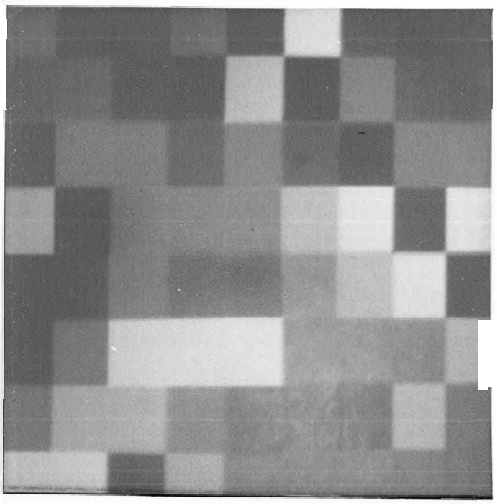

ESTPED

Appendix A

Equalized and Normalized

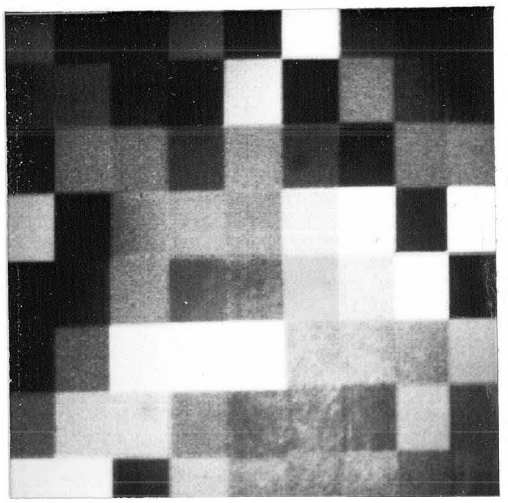

PED EQUALIZED

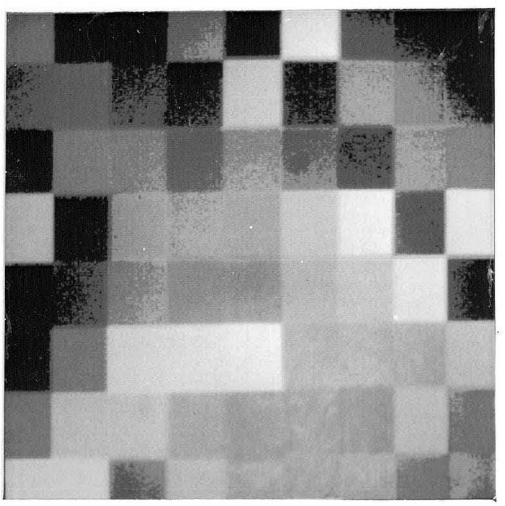

PED NORMALIZED

Appendix A

Profiles and Histograms

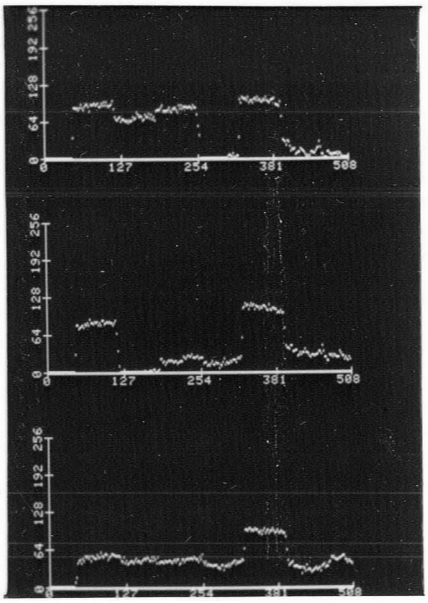

PED

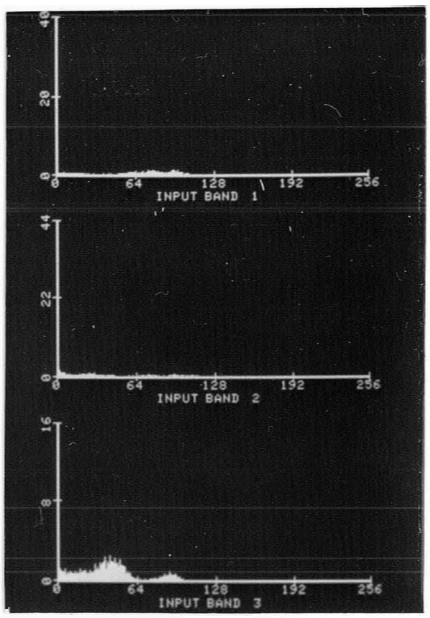

PED

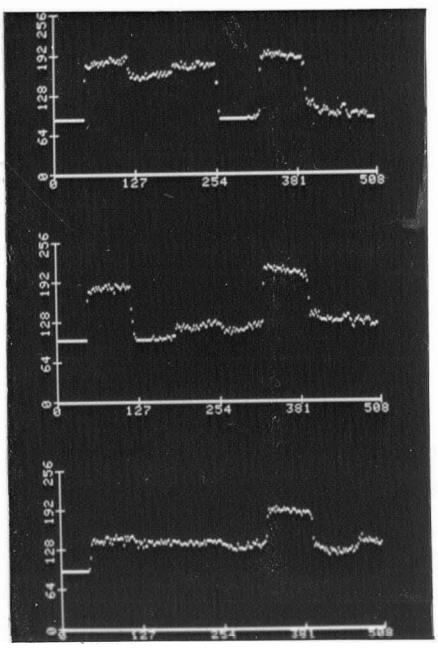

HIPED

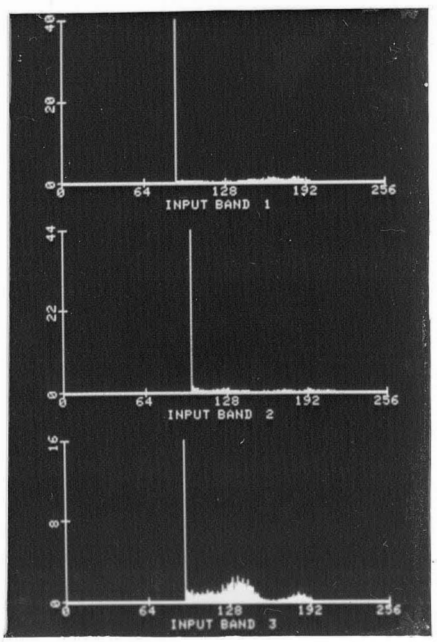

HIPED

Appendix A

Profiles and Histograms

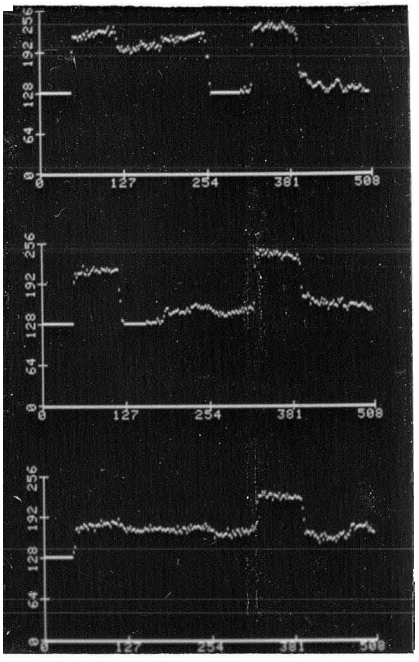

EST'PED

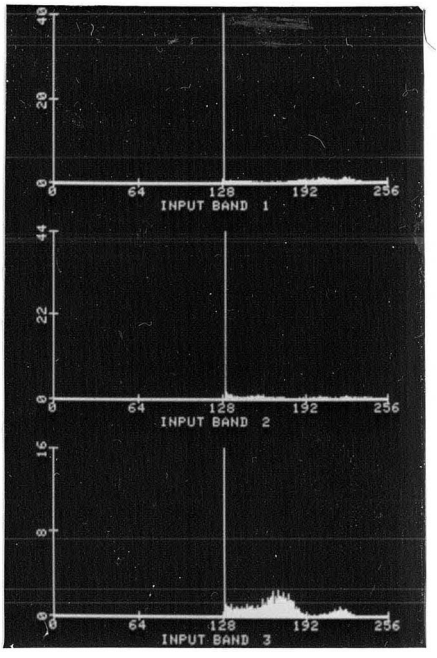

EST'PED

Appendix A

Profiles and Histograms

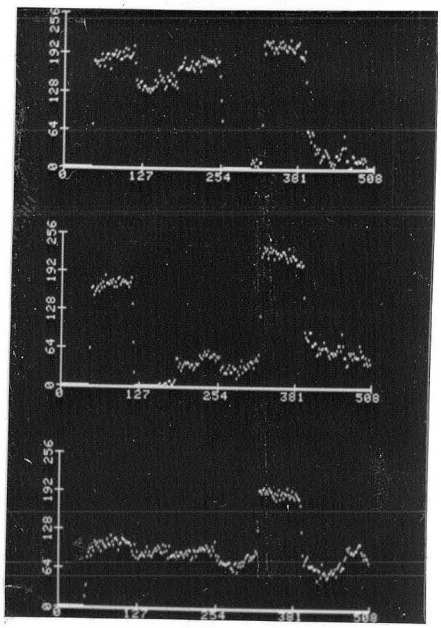

RUN 1

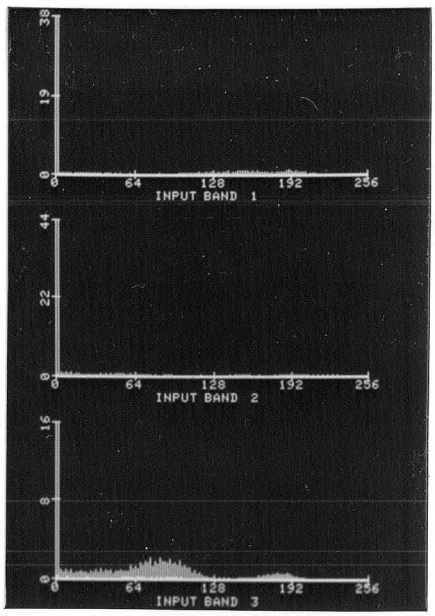

RUN 1

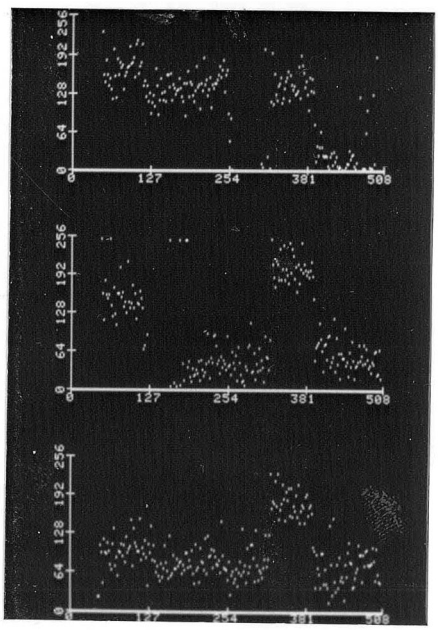

RUN 5

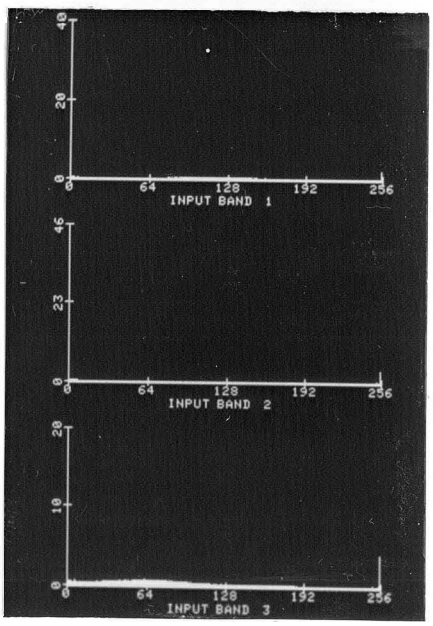

RUN 5

Appendix A

Profiles and Histograms

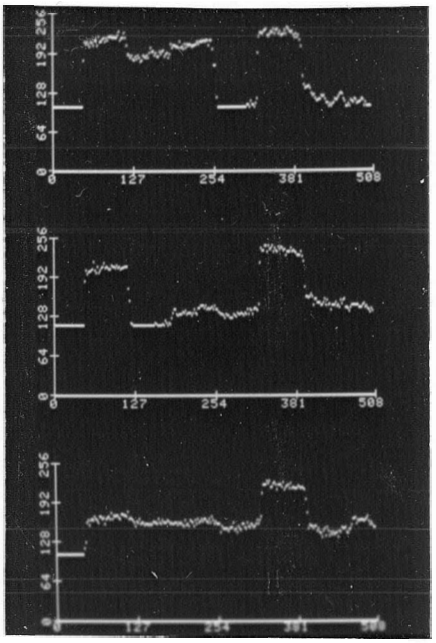

RUN 20

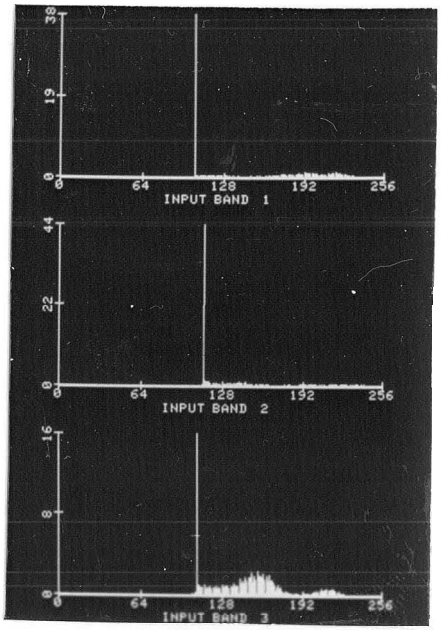

RUN 20

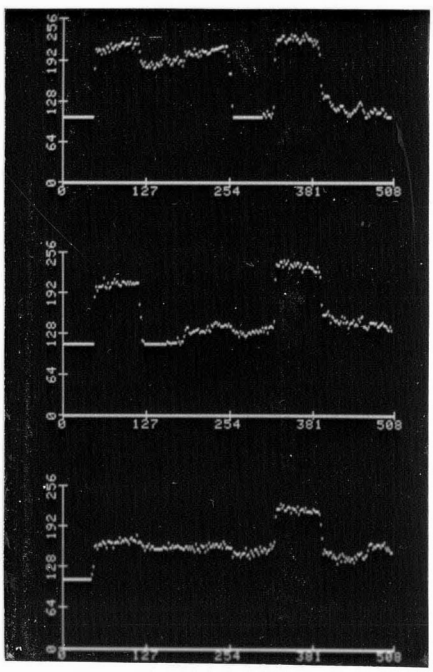

RUN 21

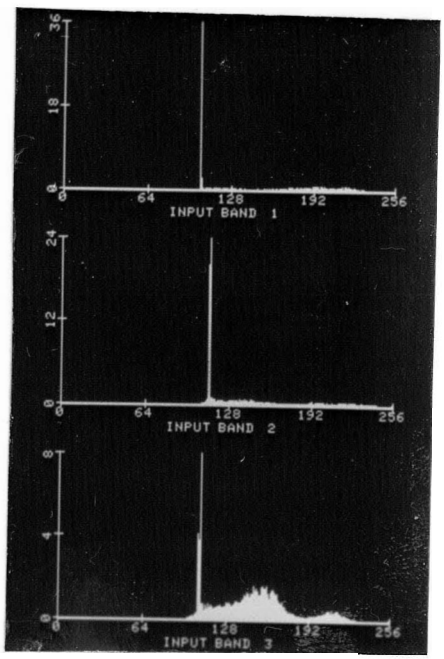

RUN 21

Appendix A

Profiles and Histograms

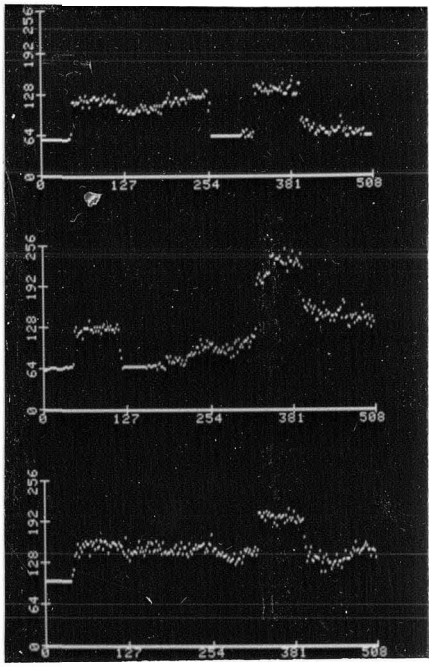

RUN 19

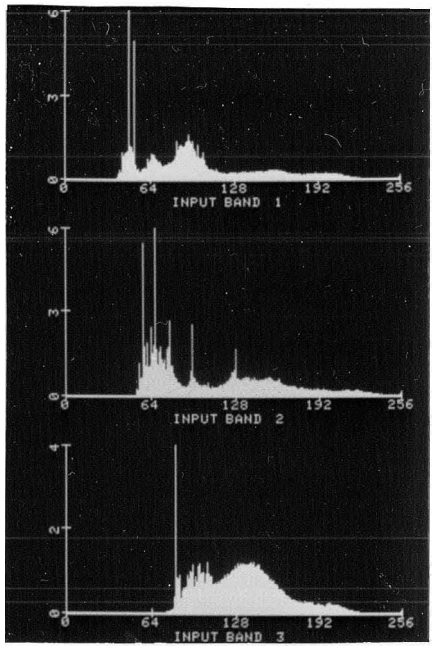

RUN 19

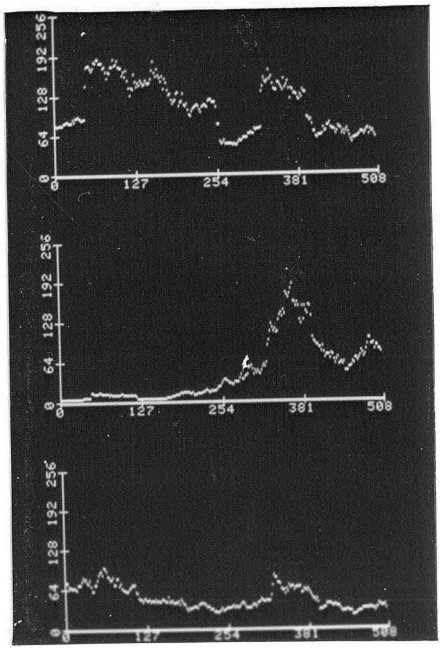

RUN 17

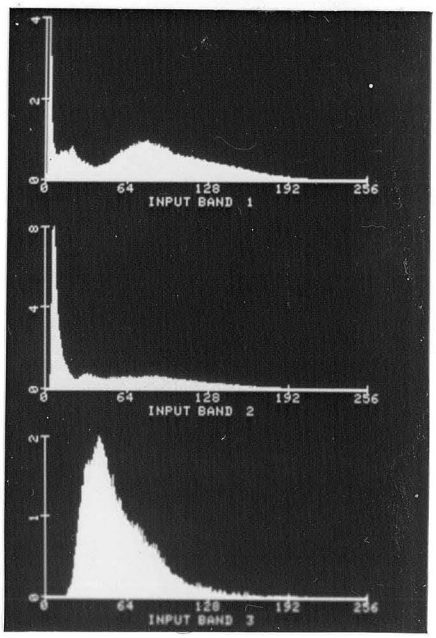

RUN 17

Appendix A

Profiles and Histograms

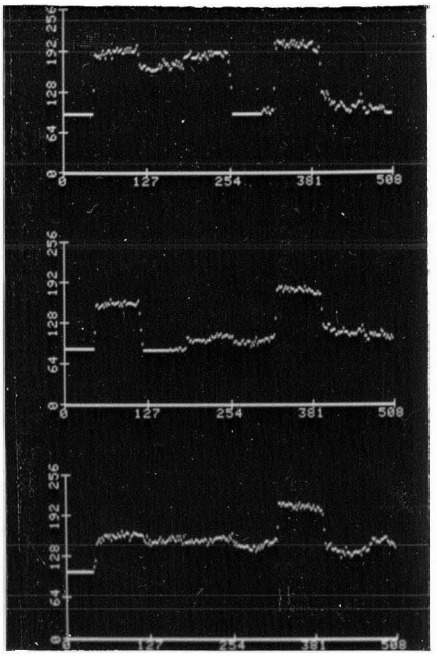

RUN 23

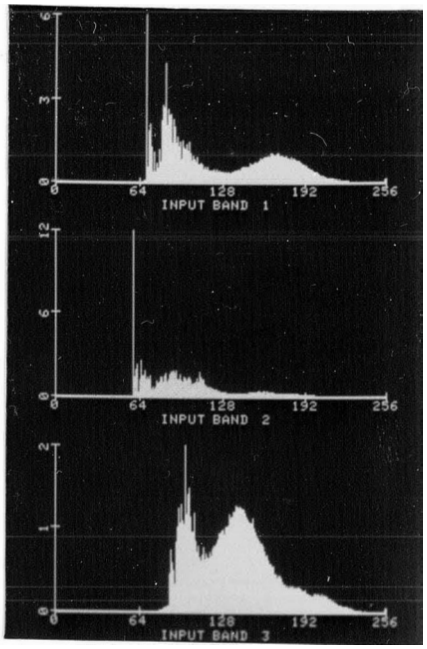

RUN 23

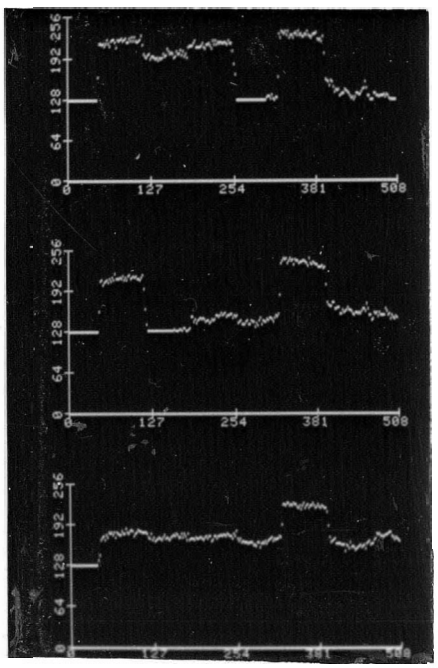

RUN 39

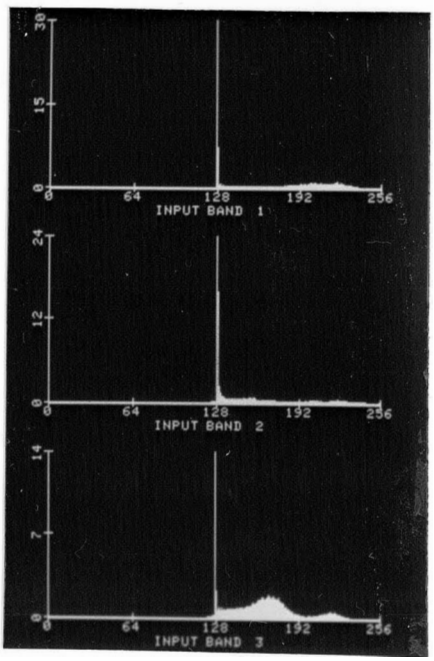

RUN 39

Appendix A

Profiles and Histograms

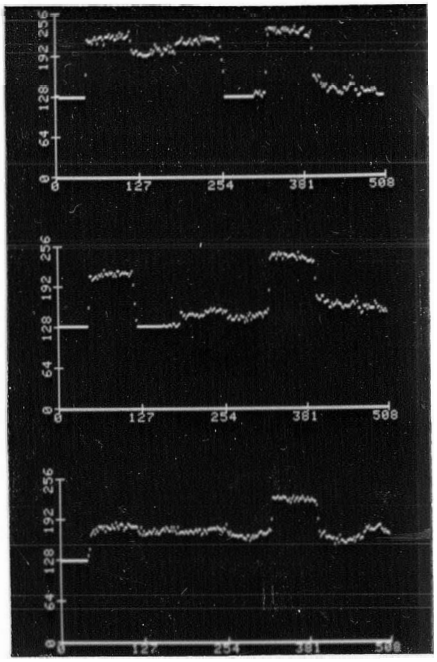

RUN 29

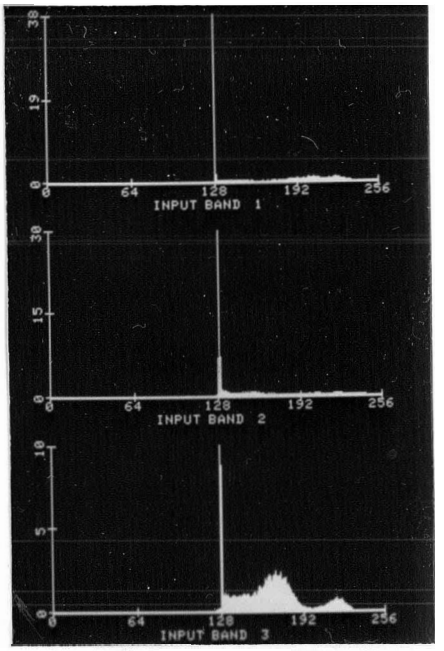

RUN 29

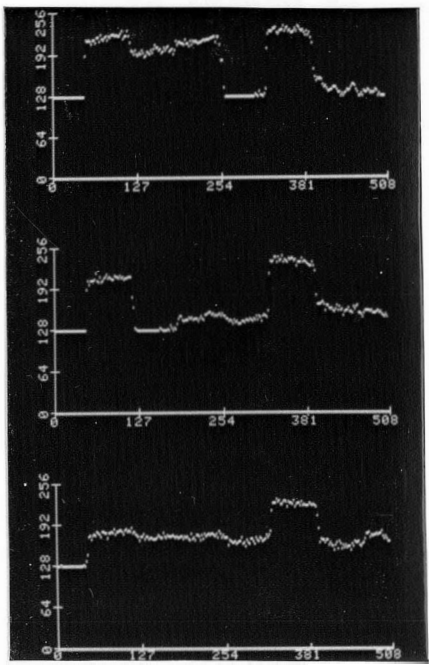

RUN 30

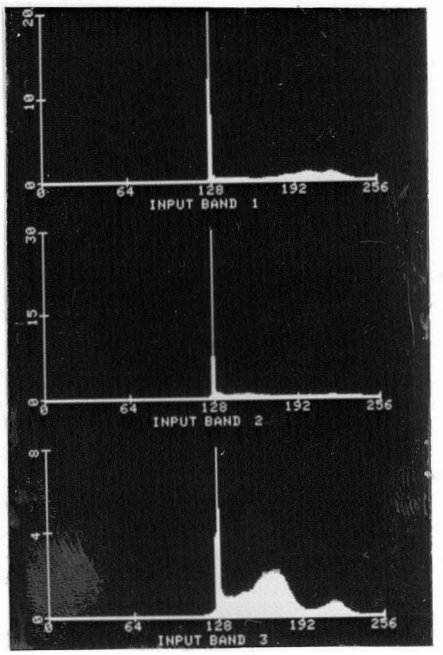

RUN 30

Appendix B

Program Rtex1_Threshold

```
      DO 200 ROW = 1, NL-1, 2
           DO 300 I = 2, NS
THRESHOLD TEST
      RED1 = IRED(ROW,I)
      RED2 = IRED(ROW,I-1)
      RATIO = RED1/RED2
      AB = ABS(RATIO-1)
      IF (AB .LT. THRESH) THEN
      B(ROW,I) = B(ROW,I-1) * RATIO
      END IF
      IF (B(ROW,I) .GT. MAX) THEN
           MAX = B(ROW,I)
           END IF
THRESHOLD TEST
      RED1 = IRED(ROW=1,NS)
      RED2 = IRED(ROW,NS)
      RATIO = RED1/RED2
      AB = ABS (RATIO-1)
      IF (AB .LT. THRESH) THEN
      B(ROW+1,NS) = B(ROW,NS)
      ELSE
      B(ROW+1,NS) = B(ROW,NS) * RATIO
```

```
      END IF
           IF (B(ROW+1,NS) .GT. MAX) THEN
                MAX = B(ROW+1,NS)
                END IF
      DO 400 I = NS-1, 1, -1
THRESHOLD TEST
      RED1 = IRED(ROW+1,I)
      RED2 = IRED(ROW+1,I+1)
      RATIO = RED1/RED2
      AB = ABS(RATIO-1)
      IF (AB .LT. THRESH) THEN
      B(ROW+1,I) = B(ROW+1,I+1)
      ELSE
      B(ROW+1,I) = B(ROW+1,I+1) * RATIO
      END IF
           IF (B(ROW+1,I) .GT. MAX) THEN
                MAX = B (ROW+1,I)
                END IF
THRESHOLD TEST
      RED1 = IRED(ROW+2,1)
      RED2 = IRED(ROW+1,1)
      RATIO = RED1/RED2
      AB = ABS(RATIO-1)
      IF (AB .LT. THRESH) THEN
      B(ROW+2,1) = B(ROW+1,1)
      ELSE
```

```
B(ROW+2,1) = B(ROW+1,1) * RATIO
END IF
     IF (B(ROW+2,1) .GT. MAX) THEN
          MAX = B(ROW+2,1)
          END IF
C(NL,1) = B(NL,1) * (255/MAX)
IBLUE2(1) = C(NL,1)
DO 600 ROW = NL, 2, -2
     DO 700 I = 2,NS
C(ROW,I) = (B(ROW,I-1) * IRED(ROW,I)/IRED(ROW,I-1))
             * 255/MAX
     IF (C(ROW,I) .GT. 255) THEN
          C(ROW,1) = 255
          END IF
IBLUE2(I) = C(ROW,I)
C(ROW-1,NS) = (B(ROW-1,NS) * IRED(ROW-1,
                NS)/IRED(ROW,NS)) * 255/MAX
     IF (C(ROW-1,NS) .GT. 255) THEN
          C(ROW-1,NS) = 255
          END IF
IBLUE2(NS) = C(ROW-1,NS)
DO 800 I = NS-1, 1, -1
C(ROW-1,I) = (B(ROW-1,I * IRED(ROW-1,
               I)/IRED(ROW-1,I+1)) * 255/MAX
     IF (C(ROW-1,I) .GT. 255) THEN
          C(ROW-1,I) = 255
```

```
          END IF
IBLUE2(I) = C(ROW-1,I)
IF(ROW .EQ. 2) GOTO 999
C(ROW-2,1) = (B(ROW-1,1) * IRED(ROW-2,
             1)/IRED(ROW-1,1) * 255/MAX
     IF (C(ROW-2,1) .GT. 255) THEN
          C(ROW-2,1) = 255
          END IF
IBLUE2(1) = C(ROW-2,1)
999 STOP
END
```

References

Bergholm, Fredrik, 1987. Edge Focusing: IEEE Transactions On Pattern Analysis And Machine Intelligence, Vol. PAMI-9, No.6, pp.726-741.

Boynton, Robert M., 1979. Human Color Vision. Holt, Rinehart and Winston, New York, U.S.A.

Brainard, David H. and Brian A. Wandell, 1986. Analysis of the retinex theory of color vision: J. Opt. Soc. Am., Vol.3, No.10, pp.1651-1661.

Brou, Philippe, Thomas R. Sciascia, Lynette Linden and Jerome Y. Lettvin, 1986. The Color of Things: Sci. Amer., Sept., pp.84-94.

Brown, P. K. and Wald, G., 1964. Visual pigments in single rods and cones of the human retina: Science, Vol.144, pp.45-52.

Buchsbaum, G., 1980. A spatial processor model for object colour perception: J. Franklin Inst., Vol.310, pp.1.

Burns Stephen A., Vivianne C. Smith, Joel Pokorny, and Anne E. Elsner, 1982. Brightness of equal-luminance lights: J. Opt. Soc. Am., Vol.72, No.9, pp.1225-1231.

Canny, John, 1986. A Computational Approach to Edge Detection: IEEE Transactions On Pattern Analysis And Machine Intelligence, Vol.PAMI-8, No.6, pp.679-698.

Chavez, Pat S., 1988. An Improved Dark-Object Subtraction Technique for Atmospheric Scattering Correction of Multispectral Data: Remote Sensing Of Environment, Vol.24, pp.459-479.

Chu, William P., 1982. Calculations of atmospheric refraction for spacecraft remote-sensing

applications: Applied Optics, Vol.22, No.5, pp.721-725.

Cornsweet, Tom N., 1970. Visual Perception: Academic Press, New York, U.S.A.

Curcio, J. A., 1961. Evaluation of atmospheric aerosol particle size distribution from scattering measurement in the visible and infrared: J. Opt. Soc. Am., Vol.51, pp.548-551.

Deschamps, P. Y., M. Herman, and D. Tanre, 1983. Modeling of the atmospheric effects and its application to the remote sensing of ocean color: Applied Optics, Vol.22, No.23, pp.3751-3758.

Diner, David J. and John V. Martonchik, 1985. Influence of Aerosol Scattering on Atmospheric Blurring of Surface Features: IEEE Transactions On Geoscience And Remote Sensing, Vol.GE-23, No.5, pp.618-624.

Evans, Ralph M., 1974. The Perception of Color. John Wiley and Sons, New York, U.S.A.

Fraser, Robert S. and Yoram J. Kaufman, 1985. The Relative Importance of Aerosol Scattering and Absorption in Remote Sensing: IEEE Transactions On Geoscience And Remote Sensing, Vol.GE-23, No.5, pp.625-633.

Funt, Brian and Jian Ho, 1988. Color From Black And White: Proceedings Of The Second International Conference On Computer Vision, The Computer Society of the IEEE, pp.2-8.

Funt, Brian V. and Mark S. Drew, 1988. Color Constancy in Near-Mondrian Scenes using a Finite Dimensional Linear Model: IEEE, The Computer Society Conference On Computer Vision And Pattern Recognition: Proceedings, pp.544-549.

Gershon, Ron, Allan D. Jepson, and John K. Tsotsos, 1987. From [R,G,B] to Surface Reflectance: Computing Color Constant Descriptors in Images: Porcroc. Of The 2ND INT. CONF. On Computer Vision DERCC. 45/88 Tampa Florida, pp.755-758.

Gordon, Howard R. and Dennis K. Clark, 1981. Clear water radiances for atmospheric correction of coastal zone color scanner imagery: Applied Optics, Vol.20, No.24, pp.4175-4180.

Graham, Clarence H., 1965. Vision and Visual Perception. John Wiley & Sons, Inc., New York, U.S.A.

Heinemann, E. G., 1955. Simultaneous brightness induction as a function inducing-and test-field luminance: J. Exptl. Psychol., Vol.50, pp.89-96.

Helson, H., 1938. Fundamental principles in color vision. I. The principle governing changes in hue, saturation, and lightness of non-selective samples in chromatic illumination: J. Exp. Psychol., Vol.23, pp.439-471.

Horn, Berthold K. P., 1974. Determining Lightness from an Image: Computer Graphics And Image Processing, Vol.3, pp.277-299.

Judd, D. B., 1940. Hue, saturation and lightness of surface colors with chromatic illumination: J. Opt. Soc. Am., Vol.30, pp.2-32.

Kaufman, Yoram J., 1981. Combined eye-atmosphere visibility model: Applied Optics, Vol.20, No.9, pp.1525-1531.

Kaufman, Yoram J., 1982. Solution of the equation of radiative transfer for remote sensing over non-uniform surface reflectivity: J. Geophys. Res. Vol.81, pp.4137-4147.

Kaufman, Yoram J., 1984. Atmospheric effects on spatial resolution of surface imagery: Applied Optics, Vol.23, No.19, pp.3400-3408.

Kaufman, Yoram J. and Robert S. Fraser, 1984. Atmospheric Effect on Classification of Finite Fields: Remote Sensing Of Environment, Vol.15, pp.95-118.

Kopeika, N. S., 1982. Spatial-frequency dependence of scattered background light: The atmospheric modulation transfer function resulting from aerosols: J. Opt. Soc. Am., Vol.72, No.5, pp.548-551.

Land, E. H., 1959. Experiments in Color Vision: Scientific American, May, pp.84-99.

Land, E. H., 1964. The Retinex: Am. Scientist, Vol.52.

Land, E. H. and McCann, John J., 1971. Lightness and Retinex Theory: J. Opt. Soc. Am., Vol.61, No.1, pp.1-11.

Land, E. H., 1977. The Retinex Theory of Color Vision: Scientific American, Dec., pp.108-128.

Land, E. H., 1983. Recent advances in retinex theory and some implications for cortical computations: color vision and the natural image: Proc. Nat. Acad. Sci., Vol.80, pp.5163-5169.

Lillesand, Thomas M. and Ralph W. Kiefer, 1979. Remote Sensing And Image Interpretation. John Wiley and Sons, New York, U.S.A.

MacAdam, D. L., 1985. Color Measurement: Themes and Variations. Springer-Verlag, Berlin.

Maloney, l., 1985. Computational approaches to color constancy, Stanford Applied Psychology Lab. Tech. Rep., Jan., Stanford University, California, U.S.A.

Maloney, Laurence T. and Brian A. Wandell, 1986. Color constancy: a method for recovering surface spectral reflectance: J. Opt. Soc. Am., Vol.3, No.1, pp.29-33.

Manual Of Remote Sensing, 1975. American Society Of Photogrammetry: First Edition, Vol.1, Robert G.Reeves, American Society of Photogrammetry, Falls Church Va., U.S.A.

Manual Of Remote Sensing, 1983. American Society Of Photogrammetry: Second Edition, Vol.1, Robert N. Colwell, The Sheridan Press, U.S.A.

Marks, W. B., Dobelle, W. H. and Macnichol, E. F., 1964. Visual pigments of single primate cones: Science, Vol.143, pp.1181.

Marr, David, 1982. Vision: A Computational Investigation into the Human Representation and Processing of Visual Information. W. H. Freeman and Company, New York, U.S.A.

McCann, J. J., S. P. McKee, and T. H. Taylor, 1976. Quantitative studies in retinex theory: a comparison between theoretical predictions and observer responses to the color Mondrian experiments: Vision Res., Vol.16, pp.445-448.

Mekler, Yuri and Yoram J. Kaufman, 1982. Contrast reduction by the atmosphere and retrieval of non-uniform surface reflectance: Applied Optics, Vol.21, No.2, pp.310-316.

Niple E., 1980. Nonlinear least squares analysis of atmospheric absorption spectra: Applied Optics, Vol.19, No.20, pp.3481-3490.

Okayama, Hiroshi and Iwao Ogura, 1983. Indicatrices of the earth's surface reflection from Landsat MSS data: Applied Optics, Vol.22, No.22, pp.3652-3656.

Overington, I. and E. P. Levin, 1971. Opt. Acta. Vol.18, pp.341.

Paritsis, N. C. and D. J. Stewart, 1983. A Cybernetic Approach to Colour Perception. Gordon And Breach Science Publishers, New York, U.S.A.

Pavlidis, Theo, 1982. Algorithms For Graphics And Image Processing, Computer Science Press Inc., U.S.A.

Pearce, William A., 1985. Cloud Shadow Effects on Remote Sensing: IEEE Transactions on Geoscience and Remote Sensing, Vol.Ge-23, No.5, pp.634-639.

Perkins, W. A., 1980. Area Segmentation of Images Using Edge Points: IEEE Transactions On Pattern Analysis And Machine Intelligence, Vol.PAMI-2, No.1, pp.8-15.

Pitas, I. and A. N. Venetsanopoulos, 1986. IEEE Transactions On Pattern Analysis And Machine Intelligence, Vol.PAMI-8, No.4, pp.538-550.

Rushton, W. A. H., 1961. The cone pigments of human fovea in colour blind and normal: Visual problems of colour, Symp.

Sjoberg, Robert W. and Berthold K.P. Horn, 1983. Atmospheric effects in satellite imaging of mountainous terrain: Applied Optics, Vol.22, No.11, pp.1702-1716.

Slater, P. N., Doyle, F. J., Fritz, N. L., and Welch R., 1983. Photographic systems for remote sensing: American Society of Photogrammetry Second Edition of Manual of Remote Sensing, Vol.1, Chap.6, pp.231-291.

Stiehl, Alan W., John J. McCann, and Robert L, Savoy, 1983. Influence of intraocular scattered light on

lightness-scaling experiments: J. Opt. Soc. Am., Vol.73, No.9, pp.1143-1148.

Terzopoulos, Demetri, 1986. Image Analysis Using Multigrid Relaxation Methods: IEEE Transactions On Pattern Analysis And Machine Intelligence, Vol.PAMI-8, No.2, pp.129-139.

Wandell, Brian A., 1987. The Synthesis and Analysis of Color Images: IEEE Transactions On Pattern Analysis And Machine Intelligence, Vol.PAMI-9, No.1, pp.2-13.

Webster's Seventh New Collegiate Dictionary, 1971. G. & C. Merriam Company, U.S.A.

Woodham, Robert J. and Malcolm H. Gray, 1987. An Analytical Method for Radiometric Correction of Satellite Multispectral Scanner Data: IEEE Transactions on Geoscience and Remote Sensing, Vol.Ge-25, No.3, pp.258-271.

Xu, H., 1983. Color-rendering capacity of illumination: J. Opt. Soc. Am., Vol.73, No.12, pp.1709-1713.